Staking, Token Pricing, and Crypto Carry*

Lin William Cong† Zhiheng He§ Ke Tang¶

First draft: Dec. 2020; this draft: June 2022

Abstract

The phenomenal rise of cryptocurrencies and decentralized finance have prominently featured "staking": Besides offering a convenience yield for transactions as digital media of exchange, tokens are frequently staked (and slashed) for base-layer consensus generation or for incentivizing economic activities and platform development, and consequently earn stakers rewards in the same tokens. To provide insights into the economics of staking and its asset pricing implications, we build a continuous-time model of a token-based economy where agents heterogeneous in wealth dynamically solve their wealth allocation (stake-transact-consume) problems. We cast the interactions as a mean field game with stochastic control and systematic shocks, which underscores aggregate staking ratio as a key variable linking staking to token pricing and equilibrium reward rate. Empirical findings on all major stakable tokens corroborate the model predictions. In particular, staking ratio has a positive correlation with reward rates in the cross section and has a negative correlation in the time series. Higher reward rates attract greater future staking, increasing an individuals' staking allocation and the staking ratio in aggregate, which in turn predicts positive excess returns. Finally, we use transaction convenience to rationalize violations of the uncovered interest rate parity and significant carry premia (e.g., a long-short carry yields a Sharpe ratio of 1.6) in the cryptocurrency data.

Keywords: Blockchain, DeFi, Proof-of-Stake, Yield Farming, Tokenomics.

*We thank Bruno Biais, Jonathan Chiu, Rod Garratt, Stephen Karolyi, Tao Li, Daniel Rabetti, Fahad Saleh, Donghwa Shin, and conference and seminar participants at the 18th Annual Conference of the Asia-Pacific Association of Derivatives, University of Cincinnati, Rizzo Center Decentralized Finance (DeFi) Conference at UNC Chapel Hill, the Fields-CFI Workshop on Mathematical Finance and Cryptocurrencies, FinTech Conference at the Fubon Center for Technology, Business and Innovation (NYU Stern), Halle Institute for Economic Research (IWH), HEC Paris, 2022 Hong Kong Conference for Fintech, AI, and Big Data in Business, Office of the Comptroller of the Currency (OCC) Novel Charters Working Group, The Pennsylvania State University Smeal College of Business, 4th Shanghai Financial Forefront Symposium, Tsinghua University PBC School of Finance, University of International Business and Economics School of Banking and Finance, the China Meeting of Econometric Society (CMES 2021, Shanghai), Ripple Labs London Onsite (Markets Team), Wolfe QES Virtual Global Innovation Conference, and Zhejiang University QingYuan Academy Digital Social Science Public Lecture Series for helpful comments and discussions. We are also grateful to the stakingrewards.com team for generously sharing the updated data that cover Sep 2020 - Feb 2022 for academic research. Corresponding contact: will.cong@cornell.edu.

†Cornell University Johnson Graduate School of Management. E-mail: will.cong@cornell.edu

§Tsinghua University. E-mail: hezh19@mails.tsinghua.edu.cn

¶Tsinghua University. E-mail: ketang@tsinghua.edu.cn

1 Introduction

The past decade witnessed the explosive growth in cryptocurrencies, which totaled 2.5 trillion USD by the end of 2021, and rising interest in Decentralized Finance (Harvey et al., 2021), which totaled over 130 billion USD as of Feb 2022. The world is also just starting to understand the categorization of tokens and their valuations as digital assets (e.g., Cong et al., 2021d; Cong and Xiao, 2021). The recent phenomenon of token staking (value locking) for higher layer DeFi innovations as well as for base layer consensus formation (e.g., through Proof-of-Stake, as discussed in John et al., 2022) further calls for a unified framework to understand the use of tokens as transaction media, investment assets, and deposit-like instruments for earning rewards.

To this end, we offer the first study relating various utility-related functions tokens provide to users (e.g., transaction convenience via medium of exchange and rewards/yield via staking) to token prices, from both theoretical and empirical angles. We start by building a continuous-time model of an economy with token-based digital networks, where agents heterogeneous in wealth optimally conduct transactions on a (blockchain) platform subject to endogenous productivity shocks, stake tokens to earn rewards from both newly minted tokens and fees, and consume off-chain. Tokens derive value by enabling users to complete economic transactions on the digital platform, making them a hybrid of money and investable assets. Stakable tokens further serve as collateral and claims to cash flows. Our model captures the following two distinguishing features of Proof-of-Stake consensus protocols and stakable projects. First, such tokens are used on platforms that support specific economic transactions or broader use in on-chain-based projects. This generates utility flows such as transaction convenience as in (Cong et al., 2021d; Biais et al., 2020). Second, the rate of staking rewards that an agent earns is influenced by other agents' behavior in aggregate, but individuals take it as given when making decisions.[1]

The equilibrium reward rate then is a fixed point determined by the whole distribution of heterogeneous agents, each solving an optimal dynamic control problem taking the mar-

[1]Polkadot (DOT) constitutes an example: the reward rate for validators is determined by the current aggregate staking ratio. The less DOTs are staked, the higher the yield is for a planned amount of reward.

ket states as given. We apply the mean field game solution to solve for the equilibrium, which marks a novel application of the methodology to economics beyond macroeconomics and inequality issues, especially with the incorporating of systemic shocks. We show that staking ratio, defined as the ratio of aggregate tokens staked in the economy to the total amount of tokens in supply, proves crucial for token pricing and reward rate determination in equilibrium. Related to the TVL (total value locked) ratio that practitioners emphasize, it constitutes a new predictor for token price dynamics. Uncovered interest rate parity (UIP) is naturally violated and our model predicts profitable trading strategies utilizing the concept of carrying. We then empirically corroborate model predictions in comprehensive data covering all major stakable tokens and DeFi projects.

Specifically, agents in our model derive utilities from consumption over an infinite horizon with a time discount. They allocate and adjust their holdings of staked tokens, tradable tokens, and numeraire under a budget constraint, trading off staking rewards, transaction convenience, and numeraire convenience for off-chain consumption. Transaction convenience endogenously increases platform productivity, which stochastically evolves, while the staking reward rate is jointly determined by aggregate reward and tokens staked. The staking ratio involves the weighted average of individual staking choices, which in turn is shaped by the agents' wealth distribution. The resulting reward rate also naturally affects agents' wealth dynamics by altering their opportunity sets. Therefore, agents' individual dynamic optimizations interact and co-evolve with the wealth distribution in a mean field game.

The resulting equilibrium is characterized by a so-called Master Equation in MFG frameworks, which captures the value function that related to individual states and also influenced by the system states with systematic shocks. The staking reward rate is determined by a fixed point problem. Token price dynamics are fully endogenous and are described by a partial differential equation akin to the Black-Merton-Scholes formula. We simplify the equation to an ordinary differential equation concerning the total token valuation, subject to intuitive boundary conditions such that tokens are worthless for unproductive platforms and are worth the entire wealth in the economy if the platform is infinitely productive.

We derive three main model implications concerning the economics of staking and its

asset pricing implications. First, the staking reward is positively related to the staking ratio in the cross section. More tokens used as rewards result in a higher staking ratio in aggregate and for individual agents. Second, the expected price appreciation increases with the aggregate staking ratio, and both the price drift and staking ratio are functions of platform productivity. Third, there are general predictable excess returns to staking over holding the numeraire, which arise as a compensation for the losses in transaction and consumption convenience.

The third implication provides a perspective that links stakable tokens and compares them to traditional assets such as currencies. The token price can be treated as an exchange rate against numeraire (such as USD), whereas the reward rate can be viewed as a deposit interest rate of the token. Then the model implies that the classical uncovered interest rate parity (UIP) fails.[2] We also derive the expression for crypto carry following the general definition of carry (Koijen et al., 2018). Higher carry (equivalent to a higher reward rate) attracts greater staking, generating excess price appreciation. As an aggregation of reward rate and price appreciation, the excess return is therefore higher. The staking reward distribution mechanically reduces the reward rate under excessive staking ratio. Consequently, carry predicts lower excess returns in the time series than in the cross-section.

For empirical analyses, we obtain data on 60 tokens from stakingrewards.com that cover all major stakable cryptocurrencies from July 2018 to February 2022. Our empirical findings support the model predictions. First, we document that a higher reward for staking significantly relates to a higher staking ratio. As the aggregate reward (relative to the total amount of tokens) increases by 0.1 units, the corresponding staking ratio increases by 7.2%. Moreover, the reward rate has a predictable effect on changes in staking ratio in both cross-section and time series. On average, a 1% increase in reward rate in the previous week increases the staking ratio in the following week by about 0.018%. This property is robust to adding both two-way fixed effect and control variables including market value effect and volatility effect. However, its significance decreases with longer time intervals, reflecting to

[2]UIP implies that the expected returns on default-free deposits across currencies are equalized, and thus the expected excess return should be zero. However, there are predictable excess returns that arise as a compensation for convenience loss. This explanation shares similar idea with Valchev (2020).

some extent the mechanical downward adjustment of the reward rate when more tokens are staked and the fact that in practice, tokens are locked for a prolonged time. An increase in staking and token locking now mechanically decrease the reward rate because the staking rewards have to be divided among more staked tokens.

We also verify in the data that a larger staking ratio predicts greater price appreciation in subsequent weeks. If the staking ratio increases by 1%, the corresponding token price will appreciate by 0.277% in the following week. Considering that the variation of staking ratio is often large, especially in the cross section, this effect is relevant for investment decisions. Crypto market return and size factors do not explain the predictive power of the staking ratio, which is closely related to market liquidity and depth, and reflects the fact that tokens can be commodity-like.[3] Staking reduces the supply of liquid cryptocurrencies, and hence pushes up the token's prices and increases the convenience yields of tokens. This is similar to how under capital constraints, using commodities as collateral for raising funds increases the spot price and the convenience yield of the underlying commodities (Tang and Zhu, 2016).

Finally, to test for violations of UIP, we follow Fama (1984)'s method and obtain that the estimated β significantly deviates from zero, and is even close to -1, where β should be zero under UIP. In a corollary, we construct a carry trade strategy that goes long high-carry crypto assets and shorts low-carry assets, yielding a Sharpe ratio of 1.61 due to that assets with higher carry generate greater returns in the cross-section. We further document how crypto carry predicts excess returns almost one-for-one in cross-section, with a reduced albeit significant effect in time series. Intuitively, a higher reward rate attracts more staking, which persists over time because tokens are typically locked for an extended period, reducing the reward rate going forward and thus the total expected return.

Our study adds to the literature on blockchain economics and cryptocurrency markets.[4]

[3]Commodities Futures Trading Commission (CFTC) regards cryptocurrencies as commodities, see, e.g., `https://www.cftc.gov/sites/default/files/2019-12/oceo_bitcoinbasics0218.pdf`.

[4]Existing studies mostly examine issues related to consensus algorithms (Biais et al., 2019; Saleh, 2021), cryptocurrency mining (e.g., Cong et al., 2021e; Lehar and Parlour, 2020), scalability (e.g., Abadi and Brunnermeier, 2018; John et al., 2020), fee designs Easley et al. (2019); Basu et al. (2019); Huberman et al. (2021), DeFi (e.g., Harvey et al., 2021; Capponi and Jia, 2021), ICOs (e.g., Lyandres et al., 2019; Howell et al., 2020), pricing of crypto assets (e.g., Liu et al., 2019; Cong et al., 2021a; Prat et al., 2019), manipulation and regulation (e.g., Griffin and Shams, 2020; Li et al., 2021; Cong et al., 2021b, n.d.), or digital currencies (e.g., Gans et al., 2015; Bech and Garratt, 2017; Chiu et al., 2019; Cong and Mayer, 2021).

In particular, we build on the tokenomics framework of Cong et al. (2021d) and Cong et al. (2021c) to add to emerging studies on Proof-of-Stake protocols (e.g., Fanti et al., 2019; Saleh, 2021; Benhaim et al., 2021) and debates on the environmental and scalability issues associated with Proof-of-Work (PoW) protocols (e.g., Cong et al., 2021e; Hinzen et al., 2019). The most closely related paper to ours is John et al. (2022) which theoretically examines native PoS crypto assets that serve primarily as investment vehicles, whereas we focus on the platform tokens with a combination of utility flow and investment function while endogenizing agents' dynamic consumption off-chain. While both studies demonstrate that the equilibrium staking ratio increases in staking rewards, John et al. (2022) finds that staked asset value can exhibit a non-monotonic relationship with block rewards and cause redistribution when agents have heterogeneous trading horizons. In contrast, we explore agents' heterogeneity in wealth and how equilibrium staking ratio predicts future price dynamics. We also examine UIP violations and crypto carry concerning the cross section of tokens, offer likely the first study of equilibrium DeFi staking to complement overviews such as Harvey et al. (2021), and provide empirical evidence to corroborate our model predictions.

A sizable literature documents uncovered interest rate parity (e.g., Fama, 1984; Lustig et al., 2019). Carry and its predictability has been analyzed not only for currencies but also for other assets such as equities (e.g., Fama and French, 1998; Griffin et al., 2003; Hou et al., 2011), bonds (e.g., Ilmanen, 1995; Barr and Priestley, 2004), and commodities (e.g., Bailey and Chan, 1993; Casassus and Collin-Dufresne, 2005; Tang and Xiong, 2012). Koijen et al. (2018) applies a general concept of carry and finds that carry predicts returns in both the cross-section and time series. We add by documenting UIP violations and carry among cryptocurrencies (and fiat currencies). We theoretically rationalize the observations and link carry to tokenomics, complementing recent empirical work by Franz and Valentin (2020) which documents deviations of covered interest parity in cryptocurrencies.

The remainder of this paper is structured as follows. Section 2 describes institutional background and stylized facts concerning staking. Section 3 proposes a dynamic model of the staking economy. Section 4 solves the model and derives implications. Section 5 presents corroborating empirical evidence. Section 6 discusses crypto carry. Section 7 concludes.

2 Institutional Background, Data, and Stylized Facts

Staking in general involves two broad categories of activities: those related to pan-PoS consensus protocols and those in higher layer DeFi applications.

2.1 Staking Mechanisms

Consensus generation in PoS. Fundamentally, blockchain functions to generate a relatively decentralized consensus to enable economic interactions such as value or information exchanges (e.g., Cong and He, 2019). Permissionless blockchains, with Bitcoin as the best-known example, have historically relied on variants of the PoW protocol. Because of scalability and environmental issues of PoW (Cong et al., 2021e; John et al., 2020), PoS protocols have gained popularity and momentum for both permissioned and permissionless blockchains, with major market players adopting and incumbents such as Ethereum contemplating a conversion (Irresberger et al., 2021).

Under PoS, agents who stake native tokens have opportunities to append blocks and earn block rewards and fees as compensation. There are mainly two ways to participate. The first is to *run a validator node, staking pool, or masternode* by holding native tokens and incurring the costs including hardware costs and time spent on maintenance. The more one stakes, the more likely one is to be selected and compensated for their participation(Saleh, 2021, contains more details). Note that holding a token does not necessarily mean participating in staking. The second way is through *delegation*. Agents only need to delegate their tokens to an existing node or a pool to receive a reward earned by the node/pool. This route is flexile and friendly for players with less tokens and allows them to share risk (Cong et al., 2021e). In practice, agents incur negligible physical costs (as opposed to the high entry cost of PoW mining or directly maintaining a node in PoS). Our study includes all protocols using pan-PoS protocols, such as Proof-of-Credit (POC) used in Nuls, which are variants of the above mechanisms.

We take Solana as a concrete example.[5] Solana is an open-source project implementing a new, high-performance, permissionless blockchain. It enables transactions to be ordered as they enter the network, rather than by block, which makes Solana one of the fastest blockchains in the world and the rapidly growing ecosystem in crypto, with thousands of projects spanning DeFi, NFTs, Web 3.0 and more. Solana uses Proof-of-Stake (PoS) as its consensus mechanism. The performance is improved by its innovative protocol, Proof-of-History (PoH). Solana's Proof of Stake is designed to quickly confirm the current sequence of transactions produced by the PoH generator, vote and select the next PoH generator, and punish misbehaving validators. A block in the context of Solana is simply the term used to describe the sequence of entries that validators vote on to achieve confirmation. *Validators* within Solana's PoS consensus model are the entities responsible for confirming if these entries are valid. *SOL* is the name of Solana's native token, which can be passed to nodes in a Solana cluster in exchange for running an on-chain program or validating its output. *Stakers* delegate SOL to validators to help increase these validators' voting weight. Such action indicates a degree of trust in the validators. Stakers delegate to ensure validators cast honest votes and hence ensure the security of the network. The more stake delegated to a validator, the more often this validator is chosen to write new transactions to the ledger, and then the more *rewards* the validator and its delegators earn.

Staking (value lockup) in DeFi. Incentivizing desirable behavior and guarding against misbehavior are crucial in DeFi applications. To this end, staking programs are popular and important in practice, which applies to a balance of tokens under custody in a smart contract. Users on DeFi platforms receive staking rewards as a form of interest payment from their token balance staked (Harvey et al., 2021). Synthetix is an example of an open-source DeFi protocol on Ethereum involving staking in its SNX tokens. Users can create and trade derivative tokens and gain exposure to assets like gold, bitcoin, and euros without having to actually own them. These derivative assets are collateralized by the platform

[5]The descriptions are basically taken from the official documentation of Solana, see `https://docs.solana.com`. We also refer to *blockdaemon.com* for some additional overviews, see `https://blockdaemon.com/platform/validator-node/how-solana-staking-works/`.

tokens (SNX) which, when locked in the contracts, enables their issuance. In return, each transaction generates a small fee distributed to SNX collateral providers. Another example is ChainLink, the leading decentralized oracle network. Oracle nodes stake LINK tokens to compete for service tasks and to ensure truthful reporting while depositors stake tokens to help with the alert system for bribery resistance and network security. In return, these agents earn staking rewards from both newly issued tokens and fees.

In practice, DeFi staking may involve different lock-up periods and multiple tokens.[6] The risks of losing the staked tokens are also different. Without getting bogged down with specific threshold requirements and operational differences across various DeFi protocols and smart contracts, DeFi staking can be characterized as simply earning rewards by collateralizing the tokens for some functionalities in the network. From the stakers' perspective, staking shares the spirit of certificates of deposit or risky illiquid investments.

Reward determination and slashing. In most staking programs, including PoS chains, on-chain projects and DeFi platforms, the total rewards used to incentivize staking or its determination mechanism are pre-specified and announced. Therefore, the aggregate reward for a specific time window is common knowledge.

In PoS, the blockchain branch is randomly selected from the whole staking pool. That is, the staking reward is randomly distributed to stakeholders based on the number of staked coins they hold as a probability weight. For example, if an investor stakes 10 coins while the aggregate staked amount of this branch is 100, then the investor has a 10% probability of appending to the branch and receiving the staking reward. As the above process continuously repeats, we can calculate the expected reward by multiplying the aggregate reward and the probability. Similarly, in DeFi platforms, stakers share the rewards from transaction fees or pre-determined emissions.

Since the rewards are yielded from staked tokens, *staking reward rate* is naturally compared to the interest rate. However, unlike deposit rates set by the banks, the staking reward rate is jointly determined by the announced staking reward and the aggregate tokens staked.

[6]MakerDAO is a good example. The profits generated from DAI can be viewed as a yield on ETH staking, and our framework can be used to understand the price impact on ETH.

Appendix E. details the staking programs for the tokens in our sample.

In addition to the opportunity costs, stakers also risk losing the staked tokens due to possible security attacks, illegal verification, and storage failure. In order to discourage validator misbehavior, most projects propose a punishment mechanism known as *slashing*. A pre-defined percentage of a validator's tokens are lost when it does not behave consistently or as expected on the network. The two prominent cases causing slashing are downtime and double signing, with the latter involving much larger penalties typically.

Market and information. In PoS, validators compete in the staked amount to earn rewards. To incentivize more delegates, they develop a reward distribution plan at the node level. Potential delegators can freely choose among these nodes or delegate through some intermediaries. Therefore, nodes engage in price competition for delegated stakes.[7] For DeFi platforms, staking reward rates are typically equal for participants, but some white-listed groups may have priority in staking. Most stakable tokens are launched on mainstream cryptocurrency exchanges. Investors can easily invest in these staking projects and trade these tokens with cryptocurrency assets such as Bitcoin and Ethereum.

Information on staking programs, including participation rules, reward distribution plan, total staked value (or total value locked, TVL, which includes non-native tokens), and even information of all the validators, are open and can be easily obtained on official websites of projects. Third party websites also specialize in collecting real-time information on staking projects; examples include *Stakingrewards.com* and *EarnCryptoInterest*. In particular, an important variable in our analysis, the *staking ratio*, which captures the total number of tokens staked as a fraction of the total number of tokens, is public knowledge.

2.2 Data

We acquire data from *Stakingrewards.com*, one of the largest websites that collect information on staking and offer both historical and real-time data of most stakable assets. Our sample covers daily observations of 60 stakable tokens with the largest market capitalization

[7] In practice, staking reward rates may not exactly equal. For example, large nodes may have slightly lower reward rates because they are considered more reliable and have more stable returns.

and longest time span, including 35 base layer pan-PoS protocols and 25 higher layer DeFi platform tokens. According to the data of the latest in-sample date (February 18, 2022), the in-sample tokens consists 93.33% of the total market capitalization of the PoS market, and 44.67% of the DeFi market. The aggregation of the two accounts for 33.06% of the total cryptocurrency market capitalization (55.08%, excludes Bitcoin).[8] The sample period covers July 2018 through Feb 2022, which overlaps with the initial birth and rapid growth of "staking."[9] Our sample covers not only the top stakable assets with the greatest market value as of the latest date (Feb 2022), but also all the stakable assets with a market value of more than 100 million US dollars as of the earlier period (Aug 2020). The additional information about staking is typically aggregated from official websites of each token, including staking participation methods, reward sharing rules, real-time staking amount (staking ratio), etc. Note that there may exist multiple staking participation methods for one token. We always choose the participation method with the lowest capital threshold and risk, such as delegating, voting, etc. Please see Appendix E. for details about staking participation.

Table 1 contains summary statistics of the tokens. In most of our analyses, we aggregate the daily observations into weekly data because daily data contains much more noise. We also aggregate data into 14-day and 30-day windows for robustness. The summary statistics show a large dispersion in the status of staking participation and price appreciation among tokens: the mean staking reward rate ranges from 0.02% to 75.20%, while the mean staking ratio ranges from 6.30% to 98.02%.

2.3 Empirical Patterns in Staking and Token Pricing

Aggregate trends. The staking economy has proliferated in recent years. First, for layer 1, the shift of focus away from PoW and onto the PoS consensus algorithms have been evident and timely.[10] The PoS share has increased substantially over time from 5% in October of

[8]The corresponding information of total market cap, PoS market cap are generated from *CoinMarketCap* and *StakingRewards.com* respectively. Among them, Ethereum is considered a stakable asset (ETH 2.0) and is contained in the 35 pan-PoS tokens.

[9]Some tokens were launched after the start date, thus the sample set is an unbalanced panel.

[10]According to 2021 Staking Ecosystem Report 2021 published by *StakingRewards* in Oct. 2021, available at `https://cms.stakingrewards.com/wp-content/uploads/2021/10/2021-Staking-Ecosystem-Report-1.pdf`.

2019 to over 20% in October 2021. As of Oct. 2021, the PoS market cap is $326.775 Billion, up from $21.117 Billion a year ago. The annual growth rate reached 1,550%, while the overall crypto market cap is up by 673%.

Meanwhile, more than 60 stakable DeFi assets, 27 masternodes and more than 50 mainstream crypto assets can be staked for rewards on DeFi platforms by the end of 2021. The entire staking economy has grown to over 4 million total users. Stakers earn a weighted-average 8% (or an equal-weighted 15%) annual staking reward rate approximately with a 40.91% weighted-average staking ratio.

Violations of uncovered interest rate parity. The Uncovered Interest Rate Parity (UIP) is an important benchmark in traditional international exchange models, especially in exchange rate determination. It implies that the difference in interest rates between two countries will equal the relative change in currency foreign exchange rates over the same period. However, UIP violation is widely documented in empirical studies (e.g., Backus et al., 1993; Engel, 1996, 2016): An increase in the domestic interest rate relative to the foreign one is associated with an increase in the excess return on the domestic currency over the foreign currency (the "UIP Puzzle"). Many explanations for the UIP violation have been proposed in previous studies, ranging from time-varying risks including liquidity and volatility risk (e.g., Bekaert, 1996; Verdelhan, 2010; Gabaix and Maggiori, 2015; Lustig et al., 2011), peso problems (e.g., Burnside et al., 2011), to time-varying convenience yield differentials (e.g., Valchev, 2020; Jiang et al., 2021).

Table 1: Summary statistics: staking reward rate, staking ratio and price change.

Token	Reward Rate, r (%, Annual)		Staking Ratio, Θ (%)		Daily Return (%)		Token	Reward Rate, r (%, Annual)		Staking Ratio, Θ (%)		Daily Return (%)	
	Mean	Std.dev.	Mean	Std.dev.	Mean	Std.dev.		Mean	Std.dev.	Mean	Std.dev.	Mean	Std.dev.
1inch	3.23	5.99	13.49	9.24	−0.39	6.32	kusama	14.14	0.79	53.58	10.81	0.52	6.38
aave	4.16	0.97	23.21	1.80	0.30	6.35	kyber	4.27	2.44	27.08	2.98	0.18	5.65
aion	6.57	1.32	26.10	3.28	0.17	6.72	livepeer	63.63	31.17	63.64	4.70	−0.27	11.48
algorand	6.54	3.10	58.01	9.15	0.03	6.03	lto	7.31	1.23	24.59	4.40	0.67	7.14
ark	9.29	0.52	54.55	1.40	−0.04	6.27	matic	24.13	12.50	24.96	3.81	0.76	7.38
avalanche	10.11	2.17	65.78	8.49	0.65	7.39	mina	12.11	1.24	98.02	4.48	−0.18	7.38
band	12.99	1.54	80.36	1.64	0.20	6.79	mirror	42.09	24.44	32.88	7.21	−0.32	6.10
bifi	8.38	3.33	47.47	15.67	0.21	6.83	near	11.98	2.01	36.77	4.40	0.45	7.14
binance-sc	12.52	5.19	67.99	12.62	0.16	4.54	nem	0.02	0.01	41.39	1.41	−0.16	4.78
bitbay	2.25	0.50	45.86	6.68	0.96	19.71	neo	2.53	1.29			0.05	5.45
cardano	5.96	2.13	66.10	10.24	0.35	5.83	nuls	9.17	0.97	44.26	4.05	0.17	6.89
cosmos	9.68	1.32	67.93	6.52	0.15	6.22	oasis	15.72	2.24	48.22	3.43	0.12	6.97
cronos	8.95	0.30	14.55	0.50	−0.60	4.91	pancakeswap	75.20	26.27	37.89	2.57	0.07	6.85
curve	3.22	1.79	73.78	19.06	0.08	7.01	peakdefi	44.14	16.63	34.66	24.78	−0.29	5.75
dash	6.28	0.28	52.45	2.45	−0.09	5.62	polkadot	12.18	1.76	60.59	5.38	0.42	6.18
decred	6.48	1.84	54.26	4.57	0.13	5.14	qtum	5.68	0.87	16.86	2.49	0.09	5.26
dfinity	15.17	2.14	49.47	0.50	−0.74	5.71	secret	26.95	2.62	49.48	4.34	0.50	7.49
dodo	67.60	4.56	42.47	3.85	−0.88	5.83	smartcash	2.49	0.53	7.77	0.77	0.12	6.40
elrond	17.91	7.00	53.42	6.88	0.64	6.33	snx	26.56	21.19	62.41	15.12	0.33	6.37
eos	4.67	3.72	38.08	23.83	0.02	5.06	solana	8.41	2.86	70.87	8.57	0.67	6.68
eth2.0	11.61	11.87	6.30	2.62	0.46	3.89	stafi	20.94	3.20	21.17	3.33	−0.04	8.12
fantom	30.30	25.39	58.27	9.77	0.66	8.79	stake-dao	22.74	9.09	34.70	4.83	−0.14	8.16
flow	9.31	1.13	57.87	10.58	−0.63	5.24	sushi	10.44	4.57	31.78	3.00	−0.35	6.44
harmony	10.54	0.77	45.29	6.03	0.59	7.38	tezos	6.58	1.39	72.36	9.21	0.05	5.76
icon	17.42	3.46	27.30	6.52	0.20	6.15	tron	3.79	1.28	24.64	5.00	0.14	5.08
idex	6.89	6.81	34.09	12.78	0.27	7.54	wanchain	8.12	0.56	24.77	1.66	0.19	6.24
injective	4.35	0.18	97.34	0.83	−0.38	6.55	waves	4.39	1.44	64.61	11.87	0.24	5.99
iotex	10.15	3.62	41.81	6.17	0.09	6.62	wax	3.00	1.95	61.08	22.38	0.29	6.05
irisnet	10.64	0.59	33.83	1.92	0.40	8.12	yearn	4.75	2.68	8.35	9.26	0.32	6.97
kava	18.66	19.30	66.36	10.89	0.32	6.30	zcoin	16.04	3.28	56.88	10.18	0.35	4.72

Notes: According to the reward distribution mechanism, there is no concept of staking ratio for *neo*.

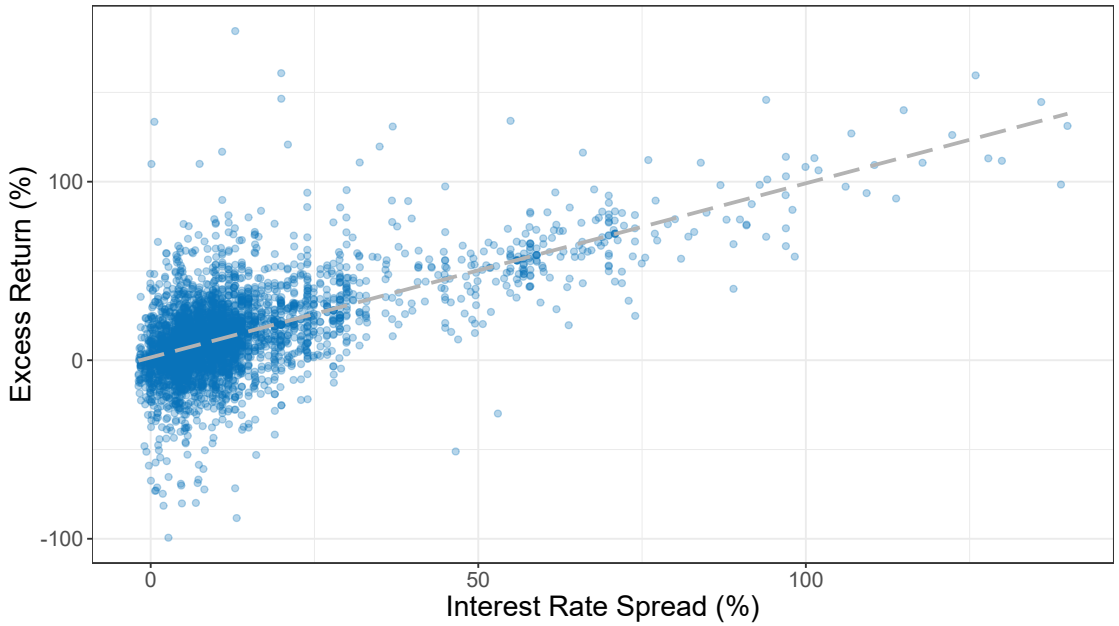

Figure 1: UIP violation in cryptocurrency markets.
This figure empirically visualizes the violation of uncovered interest rate parity (UIP) in the cryptocurrency market based on the data as Table 1 summarizes. We treat the US dollar as local currency and the 1Y treasury interest rate as the local interest rate. The data is from the Federal Reserve. For the tokens in our sample, we convert the data into weekly data. Each point in the figure indicates a weekly data point for a particular token. The staking reward rate (annualized) is used as foreign interest rate, and the x-axis, the interest rate spread, is calculated as the foreign interest rate minus the local interest rate. The y-axis is the excess return in the next week, including the interest rate spread and the price appreciation. Since the tokens are priced in US dollars, the price change is the change in foreign exchange rates. The grey line shows a linear trend of the scatter points.

We find that UIP is also violated in cryptocurrencies. Since token price and staking reward rate can be compared to exchange rates and interest rates, we can directly document crypto UIP violations. Specifically, if we treat the U.S. dollar as a local currency, then the change of token price (denominated in US dollar) is equivalently considered as the change in foreign exchange rates. Moreover, earning staking reward rates is similar to earning interest rates. Figure 1 illustrates a plot of the excess return in the next week against the interest rate spread calculated as the "foreign interest rate" minus the "local interest rate." Each blue circle in the figure indicates a weekly data point for a particular token and the grey line shows a fitted line. If UIP holds, the slope should be close to zero. However, the observed upward slope implies that an increase in the foreign interest rate relative to the local one is associated with an increase in the excess return on the cryptocurrency over the local currency, i.e., the so-called "the UIP puzzle." We discuss the implications of UIP violations

further after introducing our staking model.

3 A Dynamic Model of the Staking Economy

In our model, heterogeneous agents optimally allocate individual wealth in a continuous-time economy with a digital network subject to productivity shocks. The native token adoption and staking reward rate are endogenously determined. We capture the interaction among agents and the evolution of aggregate system states using a mean-field game (MFG for short) theoretical approach, which has been used in macroeconomics (e.g., Achdou et al., 2022), and also describing, e.g., trade crowding (Cardaliaguet and Lehalle, 2018) and mining competition (Li et al., 2019). Appendix C. introducts the theoretical background and more discussions on MFG. We also introduce an important state variable, the staking ratio, defined as the ratio of tokens staked in the economy to the total amount of tokens. It is an aggregation of the agents' controls as well as an important system state that influences token prices and agents' optimizations.

3.1 Setup

Time is continuous and infinite. A continuum of agents conducts peer-to-peer transactions on a blockchain platform or a general digital marketplace while participating in staking programs either in providing network consensus or to contribute to certain DeFi protocols. A generic consumption good serves as the numeraire and the medium of exchange on the platform is its native token.

Platform productivity and token price. As in Cong et al. (2021d), platform productivity A_t captures the general usefulness and functionality of the digital platform, and thus reflects the convenience users obtain by transacting on the platform using its tokens. We assume that A_t evolves according to a Geometric Brownian Motion:

$$\mathrm{d}A_t = \mu^A(\Theta_t)A_t\mathrm{d}t + \sigma^A A_t \mathrm{d}Z_t, \tag{1}$$

where Z_t is the primary source of uncertainty for the platform economy. Θ_t is the endogenous staking ratio, i.e., the ratio of the aggregate number of staked tokens to the total number of tokens, which will be derived later. In both the base layer (pan-PoS consensus protocols) and the higher layer (DeFi applications) staking economy, staked tokens contribute to the development of the platform by maintaining node operations, facilitating the achievement of consensus, and increasing the security level of the network, respectively. Therefore, the drift of platform productivity A_t is endogenous. We assume $\mu^A(\Theta_t)' \geqslant 0$ so that a higher staking ratio improves the platform productivity more.

Without loss of generality, we denote the token price (in numeraire) as P_t, whose dynamics follow a general diffusion process with endogenous and potentially time-varying μ_t and σ_t:

$$\mathrm{d}P_t = \mu_t P_t \mathrm{d}t + \sigma_t P_t \mathrm{d}Z_t. \tag{2}$$

Agents, adoption, and convenience. Agents of unit measure is indexed by i and each is characterized by her current wealth $w_{i,t}$. Each agent makes consumption-portfolio choices among staked (locked) tokens, non-staked (tradable) tokens, and numeraire (consumption goods or fiat). An agent becomes a platform user if she holds tokens either for staking or transactions on the platform.

Users gain convenience from holding tokens and conducting economic activities on the platform. Since staked tokens are locked from the staker's perspective, they can only derive transaction convenience from non-staked (tradable) tokens, which we model similarly as in Cong et al. (2021d,c): For an agent holding x_t (in numeraire, positive) worth of tradable tokens on the platform, she derives a utility flow:

$$\mathrm{d}v(x_t) = \mathrm{d}v_t = x_t^{1-\alpha}(u_t A_t)^{\alpha}\mathrm{d}t - \varphi \mathrm{d}t. \tag{3}$$

Even though we focus on token convenience as a medium of exchange, the reduced-form convenience could also include other utility flows such as governance and voting rights.

The marginal transaction convenience $\frac{\partial v}{\partial x} > 0$ and decreases with x_t with $\alpha \in (0,1)$. $u_t = u(w_t) > 0$ is the user type that reflects heterogeneity in transaction needs and is a

function of wealth w_t since agents only differ in w_t. At any time t, agents can choose not to participate and collect zero utility. Agents adopting the platform need to incur a flow cost φ per unit of time for platform adoption to realize the transaction convenience as the second term in Eq.(3) shows. It captures the required effort and attention for participation.

Following Bansal and Coleman (1996) and Valchev (2020), the convenience of holding the numeraire is reflected in the reduction of transaction costs in consumption. We denote the transaction cost as $\Psi_t = \Psi_t(y_t, n_t, A_t) \geqslant 0$, where y_t and n_t are consumption and numeraire holdings respectively. Naturally, $\frac{\partial \Psi}{\partial y} > 0$ and $\frac{\partial \Psi}{\partial n} < 0$. Then $-\frac{\partial \Psi}{\partial n} > 0$ reflects the marginal convenience yield of holding the numeraire. As a relative concept, the convenience of numeraire also relates to the platform. When the platform productivity is lower, the relative convenience of numeraire is higher. Thus we assume $\frac{\partial \Psi}{\partial A} < 0$.

We later specify that the token convenience and transaction costs enter agents' wealth dynamics rather than utility, for two reasons: First, token convenience flow and transaction costs are indeed in monetary form in practice, corresponding to business profits and liquidity costs on real balances respectively. Second, this approach is functionally equivalent to accounting them in the utility function (Feenstra, 1986), and is a standard approach in the literatures on convenience yields of bonds, etc.

Staking rewards. Staking rewards incentivize agents to stake their tokens to either generate consensus records in a base layer or participate in some DeFi program, such as a liquidity pool or insurance pool. In practice, staking rewards come from additional token issuance (emission) or fees others pay. The reward schedule is typically public information at the time of staking, and can be at least estimated based on real-time blockchain data (see details in Appendix E.). To quantify staking rewards, we denote the total amount of tokens at time t as Q_t, which satisfies

$$\mathrm{d}Q_t = E(Q_t, A_t)\mathrm{d}t. \tag{4}$$

We denote the aggregate rewards generated by the transaction fee by a random variable $F_t = \tau_t Q_t \geqslant 0$, the randomness can capture unexpected reward shock and volatility in

yield observed in practice.[11] If the system involves only a constant emission for rewards, then the total amount of tokens distributed as staking rewards at time t, R_t, comes from a combination of emission and fees:

$$R_t = E(Q_t, A_t) + F_t(Q_t, A_t) = \iota_t Q_t + \tau_t Q_t. \tag{5}$$

The growth rate of token supply implies an inflation rate ι_t. However, agents are not staking because holding tokens for transactions are subject to this inflation. Staked tokens are subject to the same inflation. Instead, inflation matters for allocating funds on-chain versus off-chain (assuming the numeraire does not have inflation).[12] All staked tokens are fungible and consequently all stakers face an instantaneous reward rate akin to interest rates on bank deposits:

$$r_t \equiv \frac{R_t}{L_t}, \quad \textit{where} \quad L_t \textit{ is the aggregate amount of staked tokens at } t. \tag{6}$$

To capture the cost of node operation and risk of slashing, we assume that stakers incur costs at a rate $c_t < r_t$ proportional to their staking amount.[13] Then if someone stakes k_t tokens ($k_t P_t$ dollars), by Itô's Lemma, the resulting wealth increments satisfy:

$$\mathrm{d}(k_t P_t) = k_t \mathrm{d}P_t + P_t(r_t - c_t)k_t \mathrm{d}t = (k_t P_t)[(\mu_t + r_t - c_t)\mathrm{d}t + \sigma \mathrm{d}Z_t]. \tag{7}$$

3.2 Agents' Problem and Staking as Optimal Control

At time t, an agent with wealth w_t chooses the level of consumption y_t, and holds a portfolio consisting of l_t numeraire-equivalent amount of staked tokens, x_t numeraire-equivalent

[11] We need no additional assumptions about F_t for both the theoretical and numerical analyses. In practice, the expected aggregate transaction fee weakly increases with A_t. In our baseline model, τ is a mean zero random variable. We also extend it to a random variable with non-negative mean $\bar{\tau}$, and even consider the case that $\bar{\tau}$ increases with A_t, which has little impact on the main properties in the present work.

[12] For simplicity, we do not model the various horizons for locking—the focus of John et al. (2022)—and in continuous time requires the tokens to be locked for dt. In our empirical tests, we only require agents to know the next period's reward emission.

[13] The time-varying nature of c_t captures the fact that gas fees and risks of slashing could change over time. But this is not crucial for our key economic insights.

amount of tradable tokens and n_t numeraire, where $x_t, l_t, n_t \in [0, w_t]$, $n_t = w_t - x_t - l_t$.

Let us start with a simple case that the system staking reward rate, r_t, and wealth distribution m_t are both given as system states.[14] The agent with personal wealth w_t decides the controls (y_t, x_t, l_t) to optimize discounted infinite horizon utility.

$$\max_{\{y_s, x_s, l_s\}_{s=t}^{\infty}} \mathrm{E}_t \left[\int_t^{\infty} e^{-\phi(s-t)} \mathcal{U}(y_s) \mathrm{d}s \right], \tag{8}$$

where $\mathcal{U}(y_t)$ is the agent's instant utility from consumption, which is strictly increasing and concave, and ϕ is the discount rate. Because the staked tokens cannot be traded, the agent also faces the budget constraint:

$$y_t \leqslant w_t - l_t. \tag{9}$$

The agent's wealth dynamics have to satisfy:

$$\begin{aligned} \mathrm{d}w_t &= [(x_t + l_t)\mu_t + l_t(r_t - c_t) + v_t - y_t - \Psi_t]\mathrm{d}t + (x_t + l_t)\sigma_t \mathrm{d}Z_t \\ &= f(y_t, x_t, l_t; w_t, m_t, r_t, A_t)\mathrm{d}t + g(y_t, x_t, l_t; w_t, m_t, r_t, A_t)\mathrm{d}Z_t. \end{aligned} \tag{10}$$

Define the indirect utility function as

$$J(t, w_t, A_t; m_t, r_t) = \max_{\{y_s, x_s, l_s\}_{s=t}^{\infty}} \mathrm{E}_t \left[\int_t^{\infty} e^{-\phi(s-t)} \mathcal{U}(y_s) \mathrm{d}s \right]. \tag{11}$$

We can derive the Hamilton-Jacobi-Bellman (HJB) equation:[15]

$$\phi J(t, w, A; m, r) = H(w, \frac{\partial J}{\partial w}, \frac{\partial^2 J}{\partial w^2}; m, r, A) + \mu^A A \frac{\partial J}{\partial A} + \frac{1}{2}(\sigma^A A)^2 \frac{\partial^2 J}{\partial A^2}, \tag{12}$$

[14] m_t affects the aggregation of individual variables, and therefore is involved in forming some system states such as the price drift μ_t and diffusion σ_t. We will show later the role of m_t and the determination of these two variables.

[15] Without causing confusion, we omitted the time subscript, t, for each variable.

where $H(\cdot)$ is the *generalized Hamiltonian* that defined as[16]

$$H(w,\xi,\zeta;m,r,A)=\max_{\{y,x,l\}}\left\{\mathcal{U}(y)+\xi f(y,x,l;w,m,r,A)+\frac{\zeta}{2}g(y,x,l;w,m,r,A)^2\right\}. \quad (13)$$

3.3 Dynamic Equilibrium

We now solve for a Markovian equilibrium for the mean-field game. As mentioned, we denote the density function of agents' wealth w at time t as $m_t = m_t(w_t)$. Assume all the investors have non-negative and finite wealth. m is an absolutely continuous density on the state space $W = [0, \bar{w}]$. In this section, we first formally introduce the staking ratio, Θ_t, which is endogenously given based on the m_t. Then we analyze the cross-sectional states in equilibrium, including the determination of reward rate, r_t, and the market clearing condition. Finally, we take the evolution of the wealth distribution m_t into account, and derive the dynamic equilibrium.

Staking ratio. As mentioned in Section 3.1, there is an important global variable, staking ratio Θ_t, the ratio of the aggregate number of staked tokens to the total number of tokens under the current given system states. The formula of Θ_t can be endogenously derived from the agents' perspective:

$$\Theta_t=\Theta(m_t,r_t)=\frac{L_t}{Q_t}=\frac{\int_W l(w_t,m_t,r_t,A_t)m_t\mathrm{d}w_t}{\int_W[x(w_t,m_t,r_t,A_t)+l(w_t,m_t,r_t,A_t)]m_t\mathrm{d}w_t}. \quad (14)$$

Agents make staking choices taken as given the reward rate. That is, the staking ratio is a function of the current reward rate r_t. Through the HJB equation and the continuity assumption of m, it can be shown that Θ_t is continuous in r_t. Staking ratio is important because it links individual choices with global states. It can be viewed and tracked on the public data websites such as *StakingRewards.com* or the official platform of the tokens.

[16]The *generalized Hamiltonian* is the corresponding Hamiltonian of the stochastic maximum principle as Yong and Zhou (1999) introduces in Chapter 3.2, which adds the risk adjustment, i.e., is related to the diffusion term. Its connection to the HJB equation derived through the dynamic programming approach is also introduced in Chapter 5. We adopt this notation and write HJB equation more compactly as in Eq.(12). Such a representation also facilitates the later proofs and derivations.

Therefore, Θ_t in public information at time t in practice.

Equilibrium reward rate. For simplicity, we assume that agents can always update their information about the wealth distribution after the realization of $\mathrm{d}t$, which means m_t is given and available for all the agents. This assumption entails no additional requirement of rationality for the agents, and also makes sense in practice thanks to the relatively high traceability of network addresses and their transactions. Some websites (e.g., *IntoTheBlock.com*) also provide gathered information, which makes it less difficult for agents to access it.

According to the reward distribution mechanism as Eq.(6) shows, the resulting reward rate r_t is updated by the aggregate of agents' controls, Θ_t. In equilibrium, we obtain a fixed point problem in r_t:

$$r_t = \frac{R_t}{Q_t \Theta(m_t, r_t, A_t)}. \tag{15}$$

We denote the equilibrium reward rate and staking ratio as r_t^* and $\Theta_t^* = \Theta(m_t, r_t^*, A_t)$. We naturally define ρ_t as the staking reward ratio,

$$\rho_t \equiv \frac{R_t}{Q_t} = \iota_t + \tau_t. \tag{16}$$

It indicates the number of tokens used for rewards as a percentage of the total amount of tokens on the platform. In contrast to staking reward rate in (6), ρ_t is a system state and completely independent of agents' staking activities. Since ρ_t has a one-to-one correspondence to the equilibrium r_t^*, the equilibrium staking ratio can also be represented as $\Theta(m_t, \rho_t)$, which is convenient for comparative statics, while $\Theta(m_t, r_t, A_t)$ facilitates transition analysis.[17]

Token market clearing. In aggregate, the total amount of tokens Q_t is equal to the sum of the number of an individual's personal token holdings, i.e.

$$Q_t P_t = \int_W (x_t + l_t) m_t \mathrm{d}w_t = \widehat{x_t + l_t}, \tag{17}$$

[17] In practice, ρ_t and r_t are both important characteristics in the staking economy. In most staking economies, especially most PoS chains, the aggregate reward ratio is fixed or at least can be estimated, while the staking reward rate features the actual return that agents will earn like deposit rate.

where $l_t = l(w_t, m_t, r_t, A_t)$ and $x_t = x(w_t, m_t, r_t, A_t)$ are the value of staked and non-staked (tradable) token holdings respectively, and $\widehat{x_t + l_t}$ represents (wealth weighted) average value of $x_t + l_t$, which is essentially the total wealth allocated to the platform since the agents are of a unit measure.

Combining Eq.(14) and Eq.(17), we obtain:

$$P_t L_t = P_t Q_t \Theta_t = \int_W l_t m_t \mathrm{d}w_t. \tag{18}$$

This equation is only related to the staked tokens, which can be considered as the market clearing conditions in the staking market. Naturally, the token price P_t that satisfies the market clearing condition should simultaneously clear both the staking and non-staking market. Otherwise, arbitrage opportunities arise.

The Mean-Field Game Equilibrium. Recall each agent's wealth evolves according to Eq.(10), in which Z_t stands for a systematic shock. This shock impacts all the agents and thus causes m_t to be a flow of measures (Cardaliaguet et al., 2019), or more precisely, the flow of conditional marginal measures of agents' wealth given the realization of Z_t. Such mean-field games (MFGs) with systematic shocks also appear in macroeconomics (e.g., the discrete-time heterogeneous agents models, Krusell and Smith, 1998). Just like classical MFG models, such a system can be described by a couple of PDEs, i.e., the HJB equation, and the Fokker-Planck (FP for short) equation, with two functions, the value function and the wealth density, as unknowns. The difference is the PDEs are stochastic due to the existence of the systematic shocks. However, recent studies recognize that such a system is not sufficiently convenient for analyzing complex settings (e.g., the systematic shock, and games with major player, Huang, 2010), and does not clearly show the connection with the concept of Nash equilibrium (Cardaliaguet et al., 2019). The proper analytic approach is therefore the so-called master equation (Lions, 2011), which is an infinite-dimensional equation set in the space of measures. Cardaliaguet et al. (2019), Cardaliaguet and Souganidis (2020, 2021), and Bertucci (2021) study the MFG master equation with systematic shocks theoretically, especially on the regularities of the system and the properties of the solution.

We adopt the master equation to close our model and characterize the equilibrium. Define the value function, $U = U(w, m, A) : \mathbb{R} \times \mathcal{P}^2(\mathbb{R}) \times \mathbb{R} \to \mathbb{R}$, where $\mathcal{P}^2(\mathbb{R})$ is the space of Borel probability measures on $\mathbb{R}$ with finite second-order moment. It associates the value of the game to an agent with wealth w when the wealth distribution is m and the platform productivity is A. Then $U(w, m, A)$ is the advanced version of the indirect utility function $J(t, w, A; m, r)$ as (11) defines, in which the density m is no longer a given state but a variable. According to (12), the value function is time independent. In addition, the reward rate r is determined cross-sectionally by m. Under proper assumptions that literatures have been discussed, $U(w, m, A)$ satisfies the following master equation:

$$\begin{aligned}
\phi U(w,m,A) =& H\left(w, \frac{\partial U}{\partial w}(w,m,A), \frac{\partial^2 U}{\partial w^2}(w,m,A); m, r, A\right) \\
&+ \int_{\mathbb{R}} \frac{\delta U}{\delta m}(w,m,A,y) \cdot \frac{\partial H}{\partial \xi}\left(w, \frac{\partial U}{\partial w}(y,m,A), \frac{\partial^2 U}{\partial w^2}(y,m,A); m, r, A\right) \mathrm{d}m(y) \\
&- \left[\int_{\mathbb{R}} \frac{\partial}{\partial y}\frac{\delta \hat{U}}{\delta m}(w,m,A,y)\mathrm{d}m(y) + 2\int_{\mathbb{R}} \frac{\partial}{\partial w}\frac{\delta \hat{U}}{\delta m}(w,m,A,y)\mathrm{d}m(y)\right. \\
&\quad \left. + \int_{\mathbb{R}\times\mathbb{R}} \frac{\partial^2}{\partial y \partial y'}\frac{\delta^2 \hat{U}}{\delta m^2}(w,m,A,y,y')\mathrm{d}m(y)\mathrm{d}m(y')\right] - \frac{\partial^2 \hat{U}}{\partial w^2}(w,m,A) \\
&- \left[\mu^A A \frac{\partial U}{\partial A}(w,m,A) + \frac{1}{2}(\sigma^A A)^2 \frac{\partial^2 U}{\partial A^2}(w,m,A)\right],
\end{aligned} \tag{19}$$

where $\hat{U} : \mathbb{R} \times \mathcal{P}^2(\mathbb{R}) \times \mathbb{R} \to \mathbb{R}$, $\hat{U}(w, m, A) = \frac{\partial H}{\partial \zeta}(w, \frac{\partial U}{\partial w}, \frac{\partial^2 U}{\partial w^2}; m, r, A) \cdot U(w, m, A) = \frac{1}{2} g(y^*, x^*, l^*; w, m, r, A) \cdot U(w, m, A)$. $\frac{\delta \hat{U}}{\delta m} : \mathbb{R} \times \mathcal{P}^2(\mathbb{R}) \times \mathbb{R} \times \mathbb{R} \to \mathbb{R}$, and $\frac{\delta^2 \hat{U}}{\delta m^2} : \mathbb{R} \times \mathcal{P}^2(\mathbb{R}) \times \mathbb{R} \times \mathbb{R} \times \mathbb{R} \to \mathbb{R}$ are the first and second order derivatives of $\hat{U}$ with respect to the measure m respectively. The formal definitions of these derivatives are provided in Appendix A.1.

Let us understand the intuition behind the master equation. The right hand side contains five terms. The first term is the *generalized Hamiltonian*, which plays a similar role in the HJB equation as (12) shows. The following three terms capture the impact of m_t on the forward evolution of the MFG system, which can be decomposed. Without the systematic shock, the master equation takes a simpler form which excludes all the terms involving $\hat{U}$, while the second term represents the impact of the "deterministic" changes in the wealth distribution. The systematic shock not only affect the agent directly (via the fourth term,

$\frac{\partial^2 \hat{U}}{\partial w^2}(w, m, A)$), but also change the whole situation of the system and thus affect the agent as a player in the game (via the third term). The last term represents the direct impact of the platform productivity, A_t. The derivation and requirements of solution are detailed in Appendix A.1.

The equilibrium for the whole system is characterized by the value function $U(w_t, m_t, A_t)$, agents' controls, $\{y_t, x_t, l_t\}_{t=0}^{\infty}$, and system states, $\{A_t, P_t, r_t, \Theta_t\}_{t=0}^{\infty}$, such that:

1. $U(w_t, m_t, A_t)$ satisfies the master equation (19);
2. each agent solves her optimization problem;
3. the platform productivity A_t satisfies the dynamic process in (1);
4. market clears and $\{r_t, \Theta_t\}$ solves the fixed point problem in (15).

Note that the whole system is driven by the dynamic process of platform productivity, A_t. Given the initial wealth distribution m_0 and the initial productivity A_0, the realized path of the variables may differ since it is influenced by the systematic shock.

4 Model Solution and Implications

As Section 3.3 shows, the master equation is time-independent in this discounted infinite horizon system, which implies that the value function changes in individual state and the global wealth density, but not directly in time. On the other hand, the systematic shock from A_t process renders the evolution path of density m_t stochastic. To this end, we solve the model and derive implications that hold widely under general wealth distributions.

4.1 Staking Ratio & Reward

We start by analyzing the optimal decision of a single agent. We define θ_t as agents' individual staking ratio given reward rate r_t at time t.

$$\theta_t = \theta(w_t, m_t, r_t, A_t) = \frac{l(w_t, m_t, r_t, A_t)}{x(w_t, m_t, r_t, A_t) + l(w_t, m_t, r_t, A_t)} = \frac{l_t}{q_t}, \tag{20}$$

where $q_t = q(w_t, m_t, r_t, A_t) = x_t + l_t$ is the aggregate value of individual token holding.

At the instant of decision-making, the agent takes the reward rate r_t as given, whereas according to (3), transaction convenience is related to user type. In particular, the marginal transaction convenience is decreasing with x_t, the amount of tradable token held. Naturally, the agent makes a trade-off between obtaining staking reward and transaction convenience. Intuitively, when the reward rate is higher, the agent should have a higher individual staking ratio θ_t. Moreover, for a given user type, when the agent holds very few tokens, staking should be dominated by non-staking, since the marginal transaction convenience is sufficiently high. Proposition 1 formalizes the tradeoffs.

Proposition 1. ***Optimal individual staking.*** *For an agent with wealth w_t, the optimal aggregate value of token holding q_t^* is unique and positive. The optimal individual staking ratio θ_t^* is heterogeneous with respect to agents' type u_t and satisfies*

$$\theta_t^* = \begin{cases} \max\left\{0, 1 - \left(\dfrac{1-\alpha}{r_t - c_t}\right)^{\frac{1}{\alpha}} \dfrac{A_t u_t}{q_t^*} \mathbb{I}\{u_t > u_1\}\right\}, & w_t > \left(\dfrac{1-\alpha}{r_t - c_t}\right)^{\frac{1}{\alpha}} A_t u_t, \\ 1 - \mathbb{I}\{u_t > u_2\}, & \textit{otherwise}, \end{cases} \tag{21}$$

where $\mathbb{I}\{\cdot\}$ is an indicator function, $u_1 = \frac{\varphi}{A_t}\left(\frac{r_t - c_t}{1-\alpha}\right)^{\frac{1-\alpha}{\alpha}}$, and $u_2 = \frac{\varphi}{A_t}\left(\frac{\varphi}{w_t}\right)^{\frac{1-\alpha}{\alpha}}$.

Clearly, agents with different wealth will have heterogeneous optimal individual staking ratio. However, the common denominator is that when the staking reward is greater, agents' staking ratio will also be weakly greater. (21) reflects agent's trade-off between staking reward and transaction convenience. Specifically, until the marginal transaction convenience becomes smaller than the staking reward rate, i.e., $r_t - c_t > (1-\alpha)(\frac{A_t u_t}{x_t^*})^{\alpha}$, the agent starts putting the excess token positions into the staking pool. The second row of (21) describes an unusual case that x_t^* exceeds the wealth constraint. Note that agents may choose not to participate when collecting non-positive transaction convenience. The indicator functions capture the conditions that agents choose to participate in the corresponding cases. Appendix A.2 proves and explains Proposition 1 in detail.

Substituting the agents' individual optimal choices into (14), we obtain the resulting aggregate staking ratio $\Theta(m_t, r_t, A_t)$. Intuitively, $\Theta(m_t, r_t, A_t)$ also weakly increases with reward rate r_t, but $(r_t, \Theta(m_t, r_t, A_t))$ needs to be jointly determined in equilibrium. Suppose the reward rate is higher, agents will expect a larger staking ratio, which in turn leads to a decrease in r_t. $(r_t, \Theta(m_t, r_t, A_t))$ should satisfies (15). As mentioned in Section 3.3, the equilibrium is determined by the system state, the aggregate staking reward ratio ρ_t.

Proposition 2. ***Equilibrium staking ratio.*** *Higher total staking reward ratio leads to a higher system staking ratio in equilibrium, i.e.* $\forall \rho' > \rho > 0$,

$$\Theta(m, \rho', A) \geqslant \Theta(m, \rho, A), \tag{22}$$

where $\rho = \frac{R}{Q}$ *is defined as the aggregate staking reward ratio (the number of tokens used for rewards as a percentage of the total amount of tokens).*

Proposition 2 gives a general expression on how aggregate staking reward affects staking ratio in equilibrium. For a given platform productivity A_t, as the aggregate staking reward ratio ρ_t increases, the corresponding overall staking ratio Θ increases. Note that Proposition 2 holds for any given distribution of agents' wealth $m_t(w_t)$. The result applies to both cross-sectional comparison and time series analysis. Note that a higher reward rate r_t does not necessarily lead to higher equilibrium staking ratio. Fixing the aggregate staking reward, more wealth staked implies a low reward rate.

Figure 2 visualizes the optimal staking choice of heterogeneous agents and the generation of equilibrium of the staking economy. Here we focus on comparative statics of reward rate r_t, thus the platform productivity A_t is fixed.[18] To simplify the numerical solutions and focus on our main interest, we make a further assumption about user type $u_t = u(w_t)$ here. Since the user type reflects the demand for transactions, we assume u_t increases monotonically and convexly with agent's wealth, $\frac{\partial u}{\partial w} > 0$ and $\frac{\partial^2 u}{\partial w^2} < 0$. This assumption is consistent with the reality that richer people have greater demand for the transaction. For each agent, the

[18] In fact, as A_t and Q_t given, μ_t and σ_t is determined in our model. Here we straightly substitute the corresponding value, the detailed analysis on token pricing will be discussed in later subsections.

individual staking ratio increases with reward rate. As for the comparison among crowds, the wealthier agents have a greater optimal staking ratio, since after they have put enough tokens into transactions, there is still wealth left to be used for staking.

As the blue curve in Figure 2 shows, the overall staking ratio $\Theta(m_t, r_t, A_t)$ weakly increases with staking reward rate r_t. Since Θ can be seen as a weighted average of θ, combined with Proposition 1, the above observation seems to be natural. In the grey interval, more agents enter the staking market as the reward rate increases. When the reward rate continues to increase, all the agents have entered the market and they will gradually increase the proportion of staking. The downward sloping black curve corresponds to (15). These two curves' unique intersection (the black point in the figure) gives the equilibrium (r_t^*, Θ_t^*) at time t.[19] Note that the platform productivity, A_t, influences the equilibrium not only by affecting the transaction convenience, but also by affecting the token price and its dynamics, which we discuss next.

4.2 Staking Ratio & Price Dynamics

We link staking activities to token prices. In general, the token price appreciates when more agents' wealth flows into the platform, whether it is due to high platform productivity and thus large transaction convenience, or due to greater participation in staking. We are interested in the drift term μ_t of token prices, which depends on both agents' control and wealth distribution cross-sectionally. Since many of the derivations in this section involve only the same time t, we omit the distribution state m_t, which is a given cross-sectional information for the agents under the assumption as Section 3.3 mentioned.

Since A_t is the only exogenous state variable, all endogenous variables are functions of A_t in equilibrium.[20] In addition, the exogenous token supply, Q_t, also affects the price. Denote

[19] We also test the same simulation under different wealth distribution in Appendix B.1, which suggests that the implication is robust with general distributions.

[20] In fact, some of the endogenous variables, such as m, are determined by the path $\{A_s\}_{0 \leqslant s \leqslant t}$, whereas under the assumption mentioned above, the past information is already involved in their values.

Figure 2: Individual staking decisions and equilibrium staking ratio.
This figure shows the heterogeneous individual staking decisions. For each agent, the individual staking ratio weakly increases with reward rate. As for the comparison among crowds, the agent who owns more wealth will have a greater optimal staking ratio, since after they have invested enough tokens for transaction, there are still tokens left to be used for staking. As Proposition 1 shows, the individual staking ratio curve is a piecewise function. In the grey interval, more agents enter the staking market as reward rate increases. When the reward rate continues to increase, all the agents have entered the market and they will gradually increase the proportion of staking. The blue curve is the the sum of the individual staking curve, which features the resulting overall staking ratio $\Theta(m_t, r_t)$. The downward sloping black curve draws the points that satisfies the equilibrium (15). As a result, the only intersection point formed by these two curves is the equilibrium situation (r_t^*, Θ_t^*) under the current system state. Here the system state A_t is fixed to be 1, $\rho_t = 5\%$. μ_t and σ_t are endogenously given by the states, which will be analyzed later. The selection of the parameters takes into account the reality of the staking market and relevant literature (details in Appendix D.).

$P_t = P(A_t, Q_t)$ and apply Itô's Lemma, we obtain:

$$\mathrm{d}P_t = \left[\frac{\partial P_t}{\partial A_t} A_t \mu_t^A + \frac{\partial P_t}{\partial Q_t} Q_t \iota_t + \frac{1}{2}\frac{\partial^2 P_t}{\partial A_t^2}(A_t \sigma^A)^2\right]\mathrm{d}t + \frac{\partial P_t}{\partial A_t} A_t \sigma^A \mathrm{d}Z_t. \tag{23}$$

By matching the coefficients to (2), we get:

$$\begin{aligned} \mu_t &= \frac{1}{P_t}\left[\frac{\partial P_t}{\partial A_t} A_t \mu_t^A + \frac{\partial P_t}{\partial Q_t} Q_t \iota_t + \frac{1}{2}\frac{\partial^2 P_t}{\partial A_t^2}(A_t \sigma^A)^2\right], \\ \sigma_t &= \frac{1}{P_t}\frac{\partial P_t}{\partial A_t} A_t \sigma^A. \end{aligned} \tag{24}$$

Note that $\frac{\partial P_t}{\partial Q_t}$ is negative, thus ι adds negatively to price drifts. In other words, emissions of staking rewards cause inflation in general, a concern voiced by practitioners regarding many staking programs.

For each agent with a positive optimal staked value l_t^* given r_t, the marginal benefits of staking is strictly larger than marginal transaction benefits. By the F.O.C., l_t^* satisfies:

$$0 = \left(\mu_t + r_t - c_t + \frac{\partial \Psi_t}{\partial n_t}\right)\frac{\partial U}{\partial w} + \left(\tilde{x}_t + l_t^*\right)\sigma_t^2 \frac{\partial^2 U}{\partial w^2}, \tag{25}$$

where $\tilde{x}_t = \left(\frac{1-\alpha}{r_t - c_t}\right)^{\frac{1}{\alpha}} A_t u_t$. (See details in the proof of Proposition 2 in Appendix A.3.) Since the user type is only related to user's wealth, we define Σ_t a subset of the feasible domain of wealth, W. An agent with wealth w_i will obtain a positive optimal staking choice if and only if $w_i \in \Sigma_t$. By the fixed-point dequation (15), the equilibrium staking ratio $\Theta_t > 0$, thus $\Sigma_t \neq \varnothing$. Integrating w over Σ_t and substituting into the market clearing condition (18), we obtain:

$$\begin{aligned} 0 = &\frac{1}{\sigma^2}(\mu + r - c)\int_\Sigma \frac{\partial_w U}{\partial_{ww} U} m \mathrm{d}w + \frac{1}{\sigma^2}\int_\Sigma \frac{\partial_w U}{\partial_{ww} U}\frac{\partial \Psi}{\partial n} m \mathrm{d}w \\ &+ PQ\Theta + \left(\frac{1-\alpha}{r-c}\right)^{\frac{1}{\alpha}} A \int_\Sigma u m \mathrm{d}w, \end{aligned} \tag{26}$$

where the time subscript is omitted, $\partial_w U$ and $\partial_{ww} U$ are the abbreviations of $\frac{\partial U}{\partial w}$ and $\frac{\partial^2 U}{\partial w^2}$ respectively. Then by substituting (24) and the fixed point (15) into (26), we obtain

$$\begin{aligned} 0 = &\frac{\partial P}{\partial Q} Q\iota + \frac{\partial P}{\partial A} A\mu^A + \left(\frac{\partial P}{\partial A}\right)^2 \left(\frac{I^x}{P} + \frac{Q\Theta}{I}\right)\left(A\sigma^A\right)^2 \\ &+ \frac{1}{2}\frac{\partial^2 P}{\partial A^2}\left(A\sigma^A\right)^2 + \left(\frac{\rho}{\Theta} - c + I^n\right) P, \end{aligned} \tag{27}$$

where

$$I = \int_\Sigma \frac{\partial_w U}{\partial_{ww} U} m \mathrm{d}w, \quad I^x = \frac{A}{I}\left(\frac{1-\alpha}{r-c}\right)^{\frac{1}{\alpha}} \int_\Sigma u m \mathrm{d}w, \quad I^n = \frac{1}{I}\int_\Sigma \frac{\partial \Psi}{\partial n}\frac{\partial_w U}{\partial_{ww} U} m \mathrm{d}w. \tag{28}$$

The resulting pricing equation (27) can be considered as a Black-Scholes-type partial differential equation (PDE) with the following differences.[21] First, the "theta" term in Black-

[21] The risk free rate of numeraire is normalized to zero.

Scholes equation reflecting the variation of the derivative value over time is absent in (27). Instead, the term $\frac{\partial P}{\partial Q}Q\iota$ captures the expected inflation from token issuance. Second, since A_t, the fundamental productivity that drives token price, is not tradable, the coefficient of $\frac{\partial P}{\partial A}$ is $A\mu^A$ rather than zero.[22] Third, the additional third term on the RHS originally comes from the risk term in the F.O.C. as (25) shows and features the price change risk from holding tokens. Moreover, there is a "flow" term, $(\frac{\rho}{\Theta} - c + I^n)P$, that reflects the excess gain from staking rewards offsetting the staking cost and convenience loss. Note that $\frac{\partial \Psi}{\partial n}$ is negative and represents the marginal decrease in transaction costs. Therefore, I^n is typically negative.

(27) is a partial differential equation for $P(A_t, Q_t)$, which is difficult to solve in general. Reconsidering the market clearing condition and the definition of Q_t, we find that $P(A_t, Q_t)Q_t = \widehat{x_t + l_t}$. It is actually an alternative form of (17). $\widehat{x_t + l_t}$ represents the aggregate wealth allocated to the platform and is independent of Q_t, the aggregate amount of tokens, since all the relevant variables are endogenous from A_t. Substituting the preceding equation into (27) and calculating the partial differentials, we will derive an ordinary differential equation (ODE). Moreover, based on the relationship between platform productivity and the allocated value, we provide two boundary conditions for solving this ODE.[23] Proposition 3 concludes the above results.

Proposition 3. ***Token price and dynamic.*** *P_t is separable with the representation:*

$$P_t = P(A_t, Q_t) = \frac{1}{Q_t}V(A_t), \tag{29}$$

[22] If the fundamental productivity is tradable, the coefficient of $\frac{\partial P}{\partial A}$ should be $r^f A$, where r^f is the risk free rate and is set to be zero in our model.

[23] In deriving the lower boundary condition, we make a further assumption on Ψ such that when $A_t \to 0$, $\forall y_t > 0$, $\Psi(y_t, n_t, A_t)$ is sufficiently large. This assumption captures the case that when the platform has almost zero productivity, the platform token is useless and the relative convenience of numeraire is therefore large.

where $V(A_t)$ captures the aggregate wealth allocated to the platform, and satisfies the ODE:

$$\begin{aligned} 0 = V'(A_t)A_t\mu_t^A + V'(A_t)^2\left(\frac{I^x(A_t)}{V(A_t)} + \frac{\Theta(A_t)}{I(A_t)}\right)(A_t\sigma^A)^2 + \frac{1}{2}V''(A_t)(A_t\sigma^A)^2 \\ + \left(\frac{\rho_t}{\Theta(A_t)} - c_t + I^n(A_t) - \iota_t\right)V(A_t), \end{aligned} \tag{30}$$

where I, I^x and I^n are denoted as in (28). The ODE is solved with a lower boundary condition,

$$\lim_{A_t \to 0} V(A_t) = 0, \tag{31}$$

and an upper boundary condition,

$$\lim_{A_t \to \infty} V(A_t) = \int_W w_t m_t(w_t) \mathrm{d}w_t. \tag{32}$$

The drift μ_t and diffusion σ_t in the token price dynamics in (2) are given by

$$\begin{aligned} \mu_t &= \frac{V'(A_t)}{V(A_t)}A_t\mu_t^A + \frac{1}{2}\frac{V''(A_t)}{V(A_t)}(A_t\sigma^A)^2 - \iota_t, \\ \sigma_t &= \frac{V'(A_t)}{V(A_t)}A_t\sigma^A. \end{aligned} \tag{33}$$

The economic implications of (30) are similar to our previous discussion of (27). Note that the subset of the whole crowd W, Σ, is determined by agents' trade-offs between transaction convenience and staking reward. Therefore, Σ is related to A_t that leads I, I^x and I^n to being functions of A_t. In addition, A_t the fixed point problem (15) is substituted, the equilibrium reward rate r_t is replaced by $\frac{\rho_t}{\Theta(A_t)}$. As for the boundary conditions, the lower boundary corresponds to the case that the platform is unproductive and thus attracts no users (staking rewards would be zero too), while the upper boundary represents that when A_t tends to infinity, the entire population allocates their wealth to the platform. See proof and details about the numerical solution in Appendix A.4. Agents expect the token price to appreciate when they expect higher future productivity. (33) also implies that expected inflation is reflected in the depreciation of token prices.

As Proposition 3 shows, under a fixed inflation rate, in equilibrium, the expected price

drift, μ_t, and staking ratio, Θ_t, are both functions of platform productivity, A_t. Figure 3 shows the joint dynamic of these two variables. In general, a greater staking ratio relates to higher expected price appreciation.[24]

There are two main economic driving forces. The first is the feedback effect of staking on the A_t process. As (1) and (24) show, a high staking ratio increases the productivity drift μ_t^A, and then leads to a large price drift μ_t. This mechanism illustrates the role that staking plays in the platform growth process. In PoS, the system state with a relatively high staking ratio implies a strong network of highly engaged validators, so that the consensus and confirmation are efficiently reached. As for high layer staking economy such as DeFi applications, with a certain capital value, a high staking ratio leads to a high TVL (total value locked), which is recognized as improving the security level of the platform. For both layers of the staking economy, the staking ratio positively impacts the growth of platform productivity A_t through the above mentioned paths respectively, therefore resulting in a greater drift. As a reflection of the value of the platform, the price drift increases accordingly to (24).

The second force comes directly from productivity A_t. On the one hand, μ_t declines in A_t. As A_t grows, agents allocate more wealth on the platform and less off-chain wealth, thus the potential future price appreciation is reduced, which generates the similar user-base stabilizing effect of tokens as Cong et al. (2021d). On the other hand, Θ_t also declines in A_t, since higher A_t results in larger transaction convenience. Therefore, the joint dynamic of μ_t and Θ_t represents a positive relationship. This mechanism also explains the shape when staking ratio is low. It reflects the case when A_t is so high that most on-chain wealth has already been allocated. Then the price drift tends to be mainly influenced by the inflation rate and is therefore negative.

To further understand the above two driving forces separately, we also consider the case where the staking ratio does not have a feedback effect on μ_t^A as shown by the grey dashed curve in Figure 3 shows. At equal staking ratios, the price drift μ_t is significantly smaller compared to the blue curve, especially when the staking ratio is high, which intuitively implies the impact of the second mechanism. At the same time, due to the existence of the

[24]We also test the same simulation under different wealth distribution in Appendix B.1, which suggests that the implication is robust with general distributions.

first mechanism, the grey curve still has a positive slope especially when the staking ratio is low.[25]

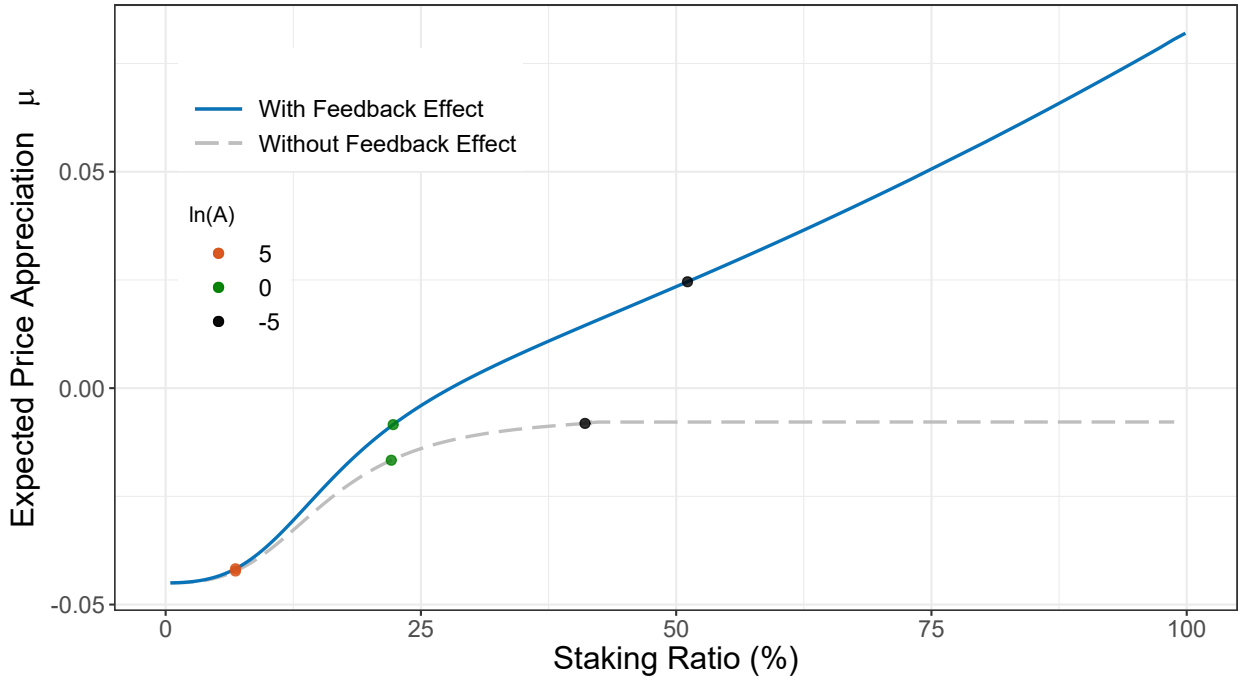

Figure 3: Staking ratio and price dynamics.
This graph shows the relationship between the system staking ratio Θ_t and the drift term of the token price μ_t. The blue curve is the case where the staking ratio feeds back the platform productivity A_t process (our main model), while the grey curve shows the case for comparison where the feedback effect does not exist. The colored scatter points on the two curves mark the corresponding point (Θ_t, μ_t) for different values of $\ln(A_t)$ respectively. As this graph shows, greater staking ratio relates to higher expected price appreciation.

4.3 Token Excess Returns & UIP Violation

For each agent, whether she holds staked tokens or non-staked tokens, she takes on the return and risk of token price fluctuation, but loses the convenience of numeraire. Denote the expected financial excess return of staked tokens over the numeraire as λ_t, then

$$\lambda_t \equiv \mathrm{E}_t\left[\mathrm{d}P_t + r^{staked\ token}\right] = \mu_t + r_t - c_t. \tag{34}$$

[25]Note that the gray curve becomes particularly flat as the staking ratio increases. It is caused by the transaction threshold φ. As A_t declines, such flow cost exceeds the transaction convenience that agents can earn. Heterogeneous agents successively cease to hold tradable tokens, thus the staking ratio rises rapidly to one. In the case of the feedback effect, given the same A_t, the staking ratio is larger (as the scatter points in Figure 3 show), even close to one, so the "flat" part is not obvious.

Proposition 4. ***Token excess return.*** *For any agent with any positive wealth, her optimal aggregate value of token holding, q_t^*, satisfies*

$$\lambda_t = -\frac{\partial \Psi}{\partial n_t} - \frac{q_t^* \sigma_t^2 \partial_{ww} U}{\partial_w U} + \frac{\min\{0, MU_x^* - MU_l^*\}}{\partial_w U}, \tag{35}$$

where $-\frac{\partial \Psi}{\partial n_t} > 0$ is the marginal convenience yield of holding numeraire, and MU_l^* and MU_x^* is marginal utility of staked and tradable tokens respectively when the agent's controls are optimized.

Proposition 4 is a fundamental property based on our model, which can be obtained directly from the optimization of agents without solving the pricing equations. (35) has been rearranged so that the left-hand side contains only λ_t, which shows that there are general predictable excess returns that arise as a compensation for convenience loss. Especially, staked token is compensated with staking rewards as financial returns for the loss of transaction convenience.

From another perspective, this is closely related to the uncovered interest rate parity (UIP) in the foreign exchange market. If we treat a token as cryptocurrency, then its price is corresponding to the concept of exchange rate, while the staking reward rate corresponds to the concept of interest rate. UIP implies that the expected returns on default-free deposits across currencies are equalized, and thus the expected excess return λ_t should be zero.[26] However, (35) shows that the uncovered interest parity does not hold, since there are predictable excess returns that arise as a compensation for convenience loss. When the convenience of numeraire increases, staked token is compensated with higher financial return. This interpretation of UIP violation shares similar ideas with Valchev (2020) 's explanation of the UIP puzzle in classical asset types. The second term on the R.H.S represents the impact of volatility risk. This correlates with the conclusions drawn from literatures that use term structure models (e.g., Bansal, 1997; Lustig et al., 2019), where the difference between domestic and foreign bond risk premia, expressed in domestic currency, is determined by

[26] In the uncovered interest rate parity among currencies, $\lambda_t = \mathrm{E}_t\left[\mathrm{d}S_t + i_t^{foreign} - i_t^{local}\right]$, where S_t is the log exchange rate (foreign currency units per unit of local currency). The corresponding terms in (34) of S_t, $i^{foreign}$ and i^{local} are respectively $\mathrm{d}P_t$, $r_t - c_t$ and the numeraire risk free rate (normalized to zero).

volatility difference of the permanent components of the stochastic discount factors. The remaining term on the R.H.S. represents the trade-off between staking and non-staking.

There are two further insights from (35). First, the excess return λ_t is a system state that can be considered exogenous when a single agent makes a decision. Second, the convenience of numeraire is a relative concept, which in fact reflects the difference in convenience between numeraire and token.

The first fact suggests that (35) also implies a trade-off between staking and non-staking by the agent. In other words, the staking reward $(r_t - c_t)$ should actually be considered as a compensation for the loss of transaction convenience. More discussion is provided in Appendix A.5. The second fact gives two important corollaries. First, even based on the same numeraire, the expected process return can be different for different tokens, since the convenience of numeraire is a relative concept. Second, not only can we use a currency such as USD as a numeraire, we can also use any of the cryptocurrencies as numeraire. Therefore, within the cryptocurrency market, UIP is violated too.

5 Empirical Analyses

In this section, we test three predictions of our model empirically: (i) Staking reward rate r_t affects agents' staking choice and thus the overall staking ratio Θ_t. (ii) Staking ratio Θ_t predicts price dynamics and token returns. (iii) Uncovered interest rate parity does not work in the cryptocurrency market.

5.1 Linking Staking Reward Rate to Aggregate Staking

Proposition 2 predicts that a higher staking reward corresponds to a higher system staking ratio in equilibrium. To test this implication empirically, we calculate the daily average of aggregate staking reward ratio and staking ratio for each token over its entire sample period. To compare different tokens, we use the concept of relative staking reward, i.e., the total amount of tokens used as staking reward divided by the total amount of issued tokens (ρ in our model). Figure 4 plots the relationship between staking reward and staking ratio,

in which each token generates one scatter point. The grey dashed line shows the linear fit of the scatters. It has a positive slope, indicating that the reward is positively related to the staking ratio. As the figure shows, most scatters are in the region where the relative reward is less than 0.15, while the other tokens might be strong influential points or "outliers". After removing these points, the linear smooth as the blue dashed line shows that the positive correlation still holds, with an even larger slope. This visualizes the implication as Proposition 2 discusses. Since the proposition is based on the equilibrium case, Figure 4 implicitly illustrates that averaging over the time series roughly conforms to the equilibrium. We also visualize the relationship with shorter data coverage (up to Oct. 2020) as Figure 4 (b) shows. Although there are fewer stakable tokens in the earlier period, the significant positive correlation between the staking ratio and staking reward ratio still exists, which suggests the relationship is robust in the sample period.

We further test the implication by panel regression. We take the staking ratio, $\Theta_{i,t}$, as a dependent variable, and the (relative) aggregate staking reward ratio, $\rho_{i,t}$, as the main explanatory variable. The variables are selected during the same period. Table 2 reports the results. As column (1) shows, the estimated coefficient of $\rho_{i,t}$ is positive and significant at a 1% level. The value of estimation implies if the aggregate reward increases by 0.1 units, then the staking ratio will increase by 0.072 (7.2%). We also test with control variables including market value and price volatility. Their potential effect is that crypto assets with greater market value are more trustworthy, making it more attractive for agents to lock in their wealth. The results show a significant impact of control variables, but neither of these two control variables affects the main effects of the staking reward ratio. We also run the regression on data with different periods and token-specific fixed effects. As Table 2 reports, the positive correlation between staking reward and staking ratio is robust.[27]

The previous test focuses on static properties in equilibrium, while from agents' perspective, the main concern is the reward rate they can earn and the resulting portfolio allocation. As Proposition 1 shows, a higher reward rate r_t will lead agents to stake more. Theoretically,

[27]To examine the robustness of the estimation to different types of tokens, we also test the main regression of Table 2 on both subsets of base layer pan-PoS tokens and higher layer DeFi platform tokens respectively (please see Appendix B.3). The results illustrate that the property apply to both the two kind of stakable tokens.

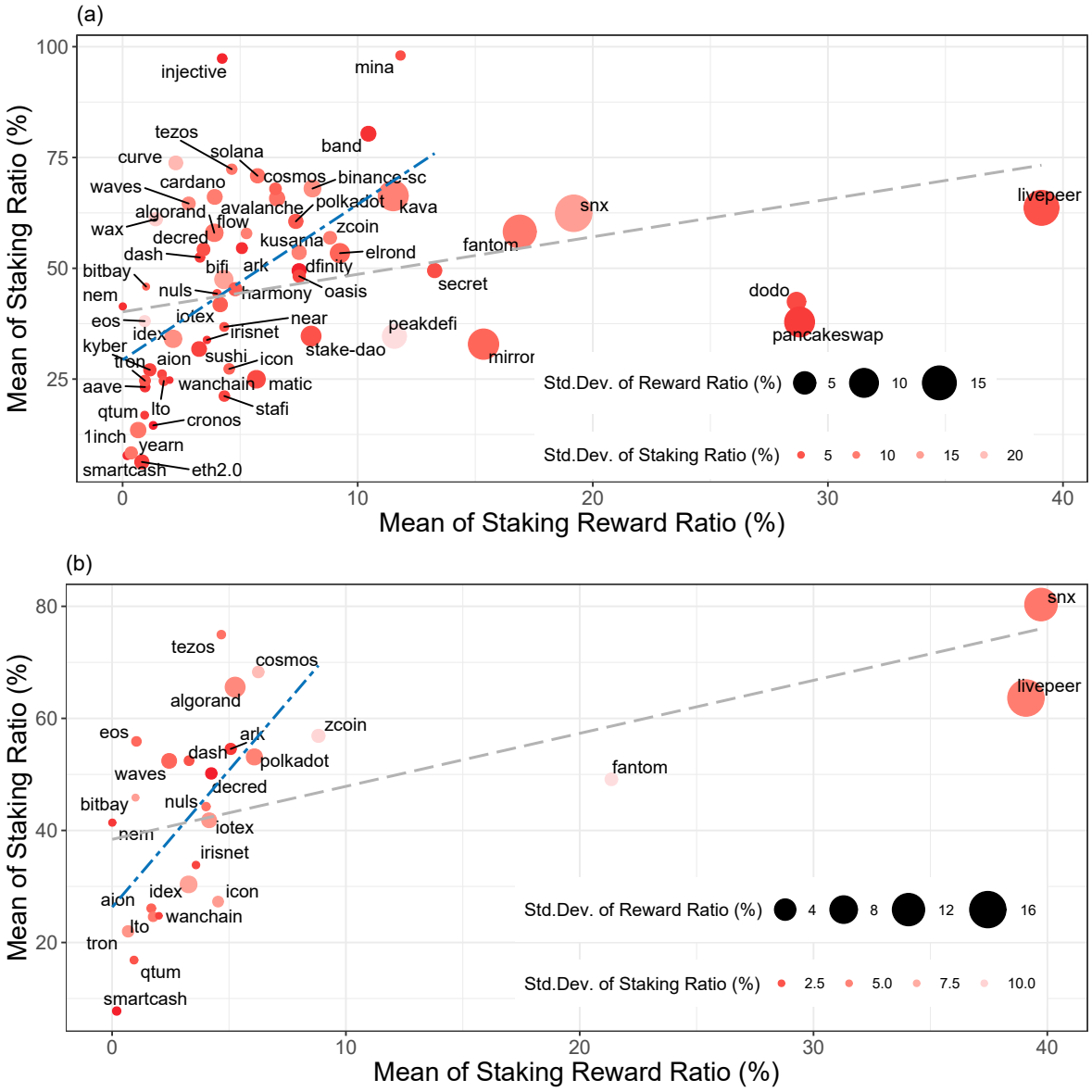

Figure 4: Staking ratio versus staking reward.

This figure plots the relationship between staking ratio Θ_t and staking reward ratio ρ_t. In panel (a), for each token, we calculate its mean staking ratio and reward over the entire time interval (up to Feb. 2022) and then generate one point. The grey dashed line is the linear regression of all scattered points, which shows a positive correlation between the two variables. After removing the influential points with large rewards, the linear regression is still upward sloping and even steeper, as shown by the blue dashed line. This plot visualizes the results of Proposition 2, i.e., a higher aggregate staking reward ratio leads to a higher system staking ratio. In addition, the size and color of the points indicate the standard deviations of the reward ratio and staking ratio respectively. In panel (b), we do the same thing with shorter data coverage (up to Oct. 2020). Although there are fewer tokens, the main relationship between the staking ratio and the staking reward ratio still holds, which implies robustness in the different sample periods.

Table 2: Staking ratio with respect to the staking reward ratio.
This table tests the relationship between staking ratio, $\Theta_{i,t}$, and the aggregate staking reward ratio, $\rho_{i,t}$, in the same period. The coefficient of $\rho_{i,t}$ is significantly positive, which implies higher staking reward results in a higher staking ratio as Proposition 2 shows. The effect is robust under multiple tests, including controls (market value and volatility), time fixed effects and different horizons (weekly, 14-day and 30-day). t-Statistics are reported in parentheses. ***,**,* indicate statistical significance at the 1%, 5% and 10% respectively.

	$StakingRatio_{i,t}$					
	7-day				14-day	30-day
	(1)	(2)	(3)	(4)	(5)	(6)
$\rho_{i,t}$	0.716***	0.758***	0.754***	0.801***	0.824***	0.825***
	(16.649)	(17.616)	(17.444)	(18.255)	(13.083)	(8.668)
$\frac{1}{100}\log(\text{Cap})_{i,t}$		1.161***	1.176***	1.702***	1.741***	1.869***
		(7.734)	(7.783)	(9.074)	(6.472)	(4.672)
$\text{Volatility}_{i,t}$			0.093	0.353***	0.517**	0.700*
			(0.878)	(2.806)	(2.429)	(1.839)
Fixed Effects						
Time				Y	Y	Y
Observations	4,009	4,009	4,009	4,009	1,981	902
R^2	0.065	0.078	0.079	0.092	0.098	0.100

the resulting high staking ratio will decrease the reward rate and evolve to equilibrium. In practice, this process takes time so that Proposition 1 generates a predictable hypothesis on the staking ratio. Empirically, we test the prediction by panel regressions as Table 3 reports.

In Table 3, we use the reward rate in the previous period, $r_{i,t-1}$, as the main independent variable, and the change in staking ratio, $\Delta\Theta_{i,t} = \Theta_{i,t} - \Theta_{i,t-1}$, as the dependent variable. The estimated coefficients of reward rate are all significantly positive, which implies a larger reward rate predicts a positive change in staking ratio. For example, as column (6) shows, if the annual reward rate increases by 1%, then the overall staking ratio will increase by 0.018% in the following week. This is a large effect considering the size of the time window and the magnitude of the change in the rewards rate in the staking economy. Market cap and token price volatility are used as control variables, since they may be related to the platform's user base and risk, thus affecting the overall staking ratio. Fixed effects are also considered. In addition, we also run the test with the staking ratio $\Theta_{i,t}$ as the dependent

variable. The estimated coefficient of reward rate is still positive and significant.[28]

[28]To examine the robustness of the estimation to different types of tokens, we also test the main regression of Table 3 on both subsets of base layer pan-PoS tokens and higher layer DeFi platform tokens respectively (please see Appendix B.3). The results illustrate that the property apply to both the two kind of stakable tokens.

Table 3: Staking ratio with respect to the staking reward rate.

This table presents the analyses of how people's staking choices are affected by the reward rate. In Panel A, we use the reward rate of the previous period, $r_{i,t-1}$ as independent. The regressions show significantly positive coefficient, which implies that larger reward rates predict the positive change of staking ratio $\Delta StakingRatio_{i,t}$. This effect is robust with controls (market value and volatility), fixed effects (token-specific effect, time effect and two-way effect), and in different horizons (weekly, 14-day and 30-day). t-Statistics are reported in parentheses. ***,**,* indicate statistical significance at the 1%, 5% and 10% respectively.

	$\Delta StakingRatio_{i,t}$							
	7-day						14-day	30-day
	(1)	(2)	(3)	(4)	(5)	(6)	(7)	(8)
$r_{i,t-1}$	0.009***	0.009***	0.009***	0.018***	0.010***	0.018***	0.028***	0.065***
	(3.193)	(3.126)	(3.234)	(3.626)	(3.508)	(3.652)	(2.901)	(3.332)
$\frac{1}{100}\log(\text{Cap})_{i,t-1}$		−0.005	−0.004	−0.053	0.020	−0.017	−0.047	−0.116
		(−0.272)	(−0.195)	(−1.270)	(0.870)	(−0.224)	(−0.316)	(−0.360)
$\text{Volatility}_{i,t-1}$			0.001	0.000	0.010	0.009	0.015	0.089
			(0.066)	(0.006)	(0.679)	(0.521)	(0.400)	(0.917)
Fixed Effects								
Token				Y		Y	Y	Y
Time					Y	Y	Y	Y
Observations	4,009	4,009	3,996	3,996	3,996	3,996	1,971	901
R^2	0.003	0.003	0.003	0.004	0.003	0.004	0.005	0.015

5.2 Equilibrium Staking Ratio and Token Price Dynamics

Our model shows that the staking ratio positively predicts token price changes. To test this prediction, we first calculate the log token price change in each period for each token, $r_{price_{i,t}} = \log(\frac{P_{i,t}}{P_{i,t-1}})$. We regress $r_{price_{i,t}}$ on the staking ratio in the previous period. As many papers have discussed, the market and market value factors have an important impact on price change, which also holds for the cryptocurrency market. Therefore, we add the current period market factor and the previous period log token market cap to the regression as controls. The calculated data for r_{MKT} is shared by Cong et al. (2021a), and the original data is collected from *CoinMarketCap.com*.

Table 4 reports the results that the staking ratio predicts price appreciation. The estimated coefficient of staking ratio is significantly positive, which implies that a higher staking ratio predicts larger token price appreciation. As column (6) shows, if the staking ratio of a token increases by 1%, its price will appreciate by 0.277% in the next week. Considering there is often a large variation in the staking ratio, this effect can have a significant impact on price. This result remains robust and significant with the addition of control variables. Therefore, the effect of price appreciation due to the staking ratio is not explained by the market and value effect. In addition, the estimated coefficients of r_{MKT} and log capitalization are consistent with related research. As Cong et al. (2021a) discusses, cryptocurrency returns exhibit network adoption premia. We also include the corresponding term, $\Delta Network_{i,t-1}$, as control, which is calculated by taking lag log differences in the total amount of addresses with non-zero balance on the platform. The estimated coefficient of the network adoption term is positive and consistent with related research. However, it does not explain the predictability of staking ratio. This suggests that the staking ratio provides incremental predictive power.[29]

[29]To examine the robustness of the estimation to different types of tokens, we also test the main regression of Table 4 on both subsets of base layer pan-PoS tokens and higher layer DeFi platform tokens respectively (please see Appendix B.3). The results illustrate that the property apply to both the two kind of stakable tokens.

Table 4: Staking ratio and token prices.

This table presents the analyses of how the staking ratio predicts token price appreciation. The main independent is the staking ratio of the previous period, $StakingRatio_{i,t-1}$. The dependent $r_{price_{i,t}}$ is the log price change. The results show that the coefficient is significantly positive, which implies that a higher staking ratio will predict higher token price appreciation. Considering that there exists market effect and market value effect in the cryptocurrency market, we also add the market price return r_{MKT_t}, the market cap term $\log(Cap)_{i,t-1}$, and the network adoption term $\Delta Network_{i,t-1}$ as controls. As Cong et al. (2021a) does, $\Delta Network_{i,t-1}$ is calculated by taking lag log differences in total amount of addresses with non-zero balance on corresponding platform. After adding these controls, the estimated coefficient of staking ratio is still significant. We also do the test in different horizons and with fixed effects to show the robustness of the results. Due to the small sample size available, we exclude the network adoption control term for the 14-day and 30-day data sets. t-Statistics are reported in parentheses. ***,**,* indicate statistical significance at the 1%, 5% and 10% respectively.

	$r_{price_{i,t}}$							
	1-day				7-day		14-day	30-day
	(1)	(2)	(3)	(4)	(5)	(6)	(7)	(8)
$StakingRatio_{i,t-1}$	0.008*	0.010**	0.031***	0.051***	0.196**	0.277*	0.444***	0.792**
	(1.899)	(2.375)	(2.834)	(2.605)	(2.532)	(1.751)	(3.204)	(2.586)
r_{MKT_t}			0.316***	0.405***	0.810***	0.821***	0.605***	0.819***
			(19.250)	(12.077)	(16.653)	(8.003)	(9.830)	(8.598)
$\log(Cap)_{i,t-1}$		−0.003***	−0.007***	−0.009***	−0.058***	−0.069***	−0.096***	−0.223***
		(−7.948)	(−6.159)	(−4.054)	(−6.951)	(−4.130)	(−6.097)	(−5.400)
$\Delta Network_{i,t-1}$				0.055***		0.035		
				(2.798)		(1.037)		
Fixed Effects								
Token	Y	Y	Y	Y	Y	Y	Y	Y
Observations	28,514	28,514	11,505	3,316	1,595	449	780	338
R^2	0.001	0.002	0.036	0.052	0.185	0.178	0.171	0.322

5.3 UIP Violation

Uncovered Interest Parity (UIP) plays a central role in exchange rate determination in most models, which implies that the expected exchange rate depreciation offsets any potential gains from interest rates. However, numerous empirical studies have shown a so-called "UIP puzzle" that an increase in the foreign interest rate relative to the local one is associated with an increase in the excess return on the foreign currency over the local currency. The popular carry trade strategy is an effective exploitation of UIP violations.

Similar phenomena arise in cryptocurrencies. Staking reward rate can be considered as interest rate, while token price can be viewed in the context of the exchange rate. Then the UIP implies that

$$\mathrm{E}_t \left[\log P_{t+1} - \log P_t\right] = r_t^f - (r_t - c_t), \tag{36}$$

where r_t^f is the local interest rate at time t.

In our model, the uncovered interest rate parity does not work in the cryptocurrency market. To empirically test if UIP works, we use the equation with some version of the original regression specification of Fama (1984) as follows:

$$\begin{aligned} \lambda_{i,t+1} &= \alpha + \beta(r_t^f - r_{i,t} + c_{i,t}) + \epsilon_{i,t+1}, \\ \text{where} \quad \lambda_{i,t} &= \log P_{i,t+1} - \log P_{i,t} + (r_{i,t} - c_{i,t}) - r_t^f, \end{aligned} \tag{37}$$

where i represents cryptocurrency i. Under UIP, $\beta = 0$, i.e. the excess return λ_t is not forecastable by the current interest rate difference. On the contrary, numerous empirical researches have found that β is not equal to 0, and even found that $\beta < 0$ so that higher interest rates are associated with higher excess returns. For the local currency, we examine in turn each asset in our sample as well as the US dollar, Bitcoin, and Ethereum. We also examine different time horizons as Valchev (2020) does.

Table 5 reports the regression results. In each row, we report the result of a specific asset as a local currency, i.e., the exchange rate of each token is converted to the price

denominated in such asset.[30] All the results show a significantly negative estimation of β, which violates the UIP. Moreover, $\beta < 0$ and is close to 1, which implies that a higher interest rate will predict a positive appreciation of the exchange rate. This leads to potential arbitrage opportunities. The regression results with different tokens as the local currency all demonstrate the UIP violation, which implies this phenomenon exists not only among the stakable tokens in our sample, but also exists when compared with traditional currencies and mainstream non-stakable cryptocurrencies.

6 Crypto Carry

As an extension of UIP violation, we test the predictability of crypto carry to token excess return and the performance of the crypto carry trade portfolio.

6.1 Carry in Other Asset Classes

Carry trades, which go long in baskets of currencies with high interest rates and short in baskets of currencies with low interest rates, have been shown to obtain high Sharpe ratios. The portfolio performance, the predictability of carry to excess returns and the possible explanation have been widely studied (e.g., Lustig et al., 2014; Bakshi and Panayotov, 2013; Burnside et al., 2011; Menkhoff et al., 2012; Koijen et al., 2018; Daniel et al., 2017).

Carry strategies are profitable for a host of different asset classes, including global equities, global bonds, commodities, US Treasuries, credit, and options. But crypto assets may differ from any traditional asset classes in terms of characteristics. On the other hand, the characteristics of the cryptocurrency market's operation may also generate new features and arbitrage opportunities (e.g., Makarov and Schoar, 2020). Therefore, carry and related contents on crypto assets may exhibit unique properties, which are discussed in recent literature (e.g., Franz and Valentin, 2020).

[30] While in principle, there are various ways to stake (e.g., delegating and running a node), which corresponds to different reward rate and costs, the staking programs mostly feature delegation/voting (that our data correspond to) which incurs negligible operational costs. We therefore normalize $c_{\{i,t\}}$ for all tokens to be zero (only their relative magnitude matters).

Table 5: Test on the UIP violation.

This table reports the panel regression results of UIP test. The regression model is shown in (37). In each row, we use a different asset as local currency and report the estimated coefficients of β with different data horizons. The estimated coeficients of β and the corresponding t-statistics are reported. All the results show significantly negative estimation of β, which proves that UIP violates. Moreover, $\beta < 0$ implies that higher interest rate will predict positive appreciation of exchange rate. The table also shows the results are consistent with the relevant research results of classic assets, and are robust among currencies and cryptocurrencies.

Local	Horizon: 7-day			Horizon: 30-day			Local	Horizon: 7-day			Horizon: 30-day		
Currency	Coef., β	t-statistic	R^2	Coef., β	t-statistic	R^2	Currency	Coef., β	t-statistic	R^2	Coef., β	t-statistic	R^2
Currency & mainstream cryptocurrencies.													
US Dollar	−0.98	(−51.18)	0.40	−0.91	(−11.18)	0.12	Ethereum	−0.99	(−59.33)	0.47	−0.95	(−13.57)	0.17
Bitcoin	−0.99	(−59.97)	0.47	−0.96	(−14.10)	0.18							
Cryptocurrencies in our sample.													
1inch	−0.98	(−34.48)	0.49	−0.83	(−6.13)	0.15	kusama	−1.01	(−39.96)	0.35	−1.09	(−11.79)	0.17
aave	−1.01	(−39.60)	0.42	−0.99	(−8.22)	0.15	kyber	−1.01	(−23.59)	0.34	−0.98	(−4.55)	0.10
aion	−0.97	(−25.11)	0.39	−0.80	(−5.29)	0.12	livepeer	−1.01	(−25.23)	0.34	−0.85	(−4.46)	0.07
algorand	−0.98	(−54.37)	0.44	−0.94	(−14.08)	0.19	lto	−1.05	(−18.80)	0.31	−0.98	(−5.82)	0.18
ark	−0.99	(−35.63)	0.50	−0.91	(−9.27)	0.24	matic	−0.96	(−31.22)	0.26	−0.90	(−6.33)	0.06
avalanche	−1.03	(−36.32)	0.37	−1.12	(−8.69)	0.13	mina	−1.00	(−32.52)	0.43	−0.82	(−6.27)	0.12
band	−1.03	(−43.19)	0.41	−1.02	(−10.94)	0.17	mirror	−0.98	(−34.24)	0.47	−0.97	(−6.58)	0.15
bifi	−0.98	(−34.86)	0.39	−0.93	(−6.93)	0.11	near	−1.01	(−40.87)	0.41	−1.01	(−9.59)	0.15
binance-sc	−0.99	(−46.09)	0.53	−0.93	(−8.74)	0.16	nem	−0.97	(−31.70)	0.58	−0.79	(−8.02)	0.29
bitbay	−0.95	(−7.94)	0.12	−1.36	(−3.64)	0.34	neo	−1.00	(−33.50)	0.46	−0.89	(−8.82)	0.21
cardano	−0.98	(−44.74)	0.44	−0.99	(−10.66)	0.16	nuls	−1.01	(−28.55)	0.43	−0.96	(−6.88)	0.17
cosmos	−0.99	(−55.48)	0.44	−0.95	(−12.86)	0.16	oasis	−0.99	(−33.92)	0.40	−0.92	(−6.93)	0.12
cronos	−0.99	(−18.04)	0.44	−1.00	(−3.34)	0.13	pancakeswap	−0.99	(−40.20)	0.46	−0.90	(−8.64)	0.15
curve	−1.00	(−39.38)	0.46	−0.94	(−9.74)	0.19	peakdefi	−0.96	(−32.93)	0.35	−0.85	(−8.15)	0.13
dash	−0.98	(−33.09)	0.47	−0.79	(−5.73)	0.11	polkadot	−1.02	(−47.82)	0.46	−1.07	(−11.48)	0.18
decred	−0.99	(−56.13)	0.45	−0.97	(−13.41)	0.17	qtum	−0.98	(−38.14)	0.55	−0.88	(−10.01)	0.28
dfinity	−0.94	(−21.14)	0.42	−0.92	(−4.03)	0.12	secret	−1.03	(−39.35)	0.39	−1.15	(−8.96)	0.13
dodo	−0.91	(−24.74)	0.41	−0.84	(−5.52)	0.12	smartcash	−0.99	(−26.26)	0.39	−0.83	(−6.80)	0.16
elrond	−1.01	(−42.05)	0.43	−1.07	(−9.39)	0.14	snx	−1.03	(−51.53)	0.42	−1.08	(−12.42)	0.15
eos	−0.99	(−51.96)	0.44	−0.92	(−11.97)	0.15	solana	−0.97	(−34.07)	0.38	−0.93	(−7.59)	0.12
eth2.0	−1.01	(−52.99)	0.47	−1.03	(−12.10)	0.17	stafi	−1.00	(−32.92)	0.32	−0.98	(−8.12)	0.12
fantom	−0.99	(−30.42)	0.21	−1.06	(−8.76)	0.09	stake-dao	−0.95	(−16.12)	0.21	−0.84	(−3.10)	0.05
flow	−0.94	(−27.02)	0.42	−0.81	(−5.57)	0.12	sushi	−0.98	(−40.90)	0.46	−0.91	(−9.86)	0.18
harmony	−0.98	(−37.27)	0.32	−0.93	(−6.18)	0.06	tezos	−1.00	(−58.16)	0.46	−0.94	(−13.01)	0.16
icon	−0.97	(−31.45)	0.45	−0.85	(−7.19)	0.17	tron	−0.98	(−58.00)	0.47	−0.91	(−12.58)	0.16
idex	−1.00	(−41.23)	0.36	−0.96	(−9.47)	0.12	wanchain	−0.98	(−26.84)	0.43	−0.90	(−7.90)	0.23
injective	−0.94	(−24.59)	0.39	−0.86	(−5.50)	0.13	waves	−0.99	(−52.10)	0.42	−0.95	(−12.33)	0.15
iotex	−0.98	(−29.49)	0.40	−0.85	(−6.91)	0.14	wax	−0.98	(−31.26)	0.27	−1.02	(−6.15)	0.07
irisnet	−1.00	(−27.01)	0.39	−0.97	(−7.42)	0.18	yearn	−1.00	(−38.09)	0.36	−0.97	(−8.80)	0.12
kava	−1.00	(−47.26)	0.41	−0.96	(−10.58)	0.14	zcoin	−0.99	(−24.69)	0.37	−0.87	(−6.69)	0.16

One of the direct corollary to the violation of UIP is the existence of carry. Koijen et al. (2018) define carry as a general concept of any asset. For any asset, carry is defined as its futures return, assuming that price stays the same, i.e.

$$\text{return} \equiv \text{carry} + \text{E(price appreciation)} + \text{unexpected price shock.} \tag{38}$$

For example, the classic definition of currency carry is the local interest rate in the corresponding country. Following Koijen's general definition of carry, we derive crypto carry based on our model as (39) shows, which is close to the form of currency carry.[31]

$$\text{carry}_t \equiv \frac{r_t - c_t - r^f}{1 + r^f}. \tag{39}$$

Table 6 summarizes annualized carry and excess return of all the tokens in our sample. Sample means and standard deviations are reported. We also include the US Dollar as one of the assets for which the carry and excess return are, by definition, equal to zero.

6.2 Crypto Carry Trade Portfolio Returns

Tokens in the asset pool are ordered by their carry in the previous period, and then divided into three groups, i.e. the top $x\%$ of assets, the bottom $x\%$ and the middle group. Then we construct a carry trade portfolio by going long high carry group with equal weight and going short low with equal weight at the end of each week. For long tokens, we also stake them to earn staking reward rate, while for the short assets, we also compensate for the staking reward rate. The choice of x does not affect our observation of the main characteristics of the carry trade portfolio. The portfolio is rebalanced every week.[32] Considering the abnormal fluctuation of token price and staking ratio when a staking project is first launched, our weekly asset pool does not include new staking projects that come out within

[31]This formula is derived based on the assumption that covered interest rate parity holds, where Koijen et al. (2018) also claim this assumption when obtaining the formula of currency carry.

[32]We also assume that the staking rules allow a one-week stake period. Most stakable tokens do offer such flexible staking options, and our data of reward rate are also selected in the corresponding options. For some rare exceptions, we can assume the existence of some derivatives that would enable such an asset allocation. Such derivatives are gradually appearing in practice.

Table 6: Excess return and carry.

Token	Excess Return (%, Annual)		Carry (%, Annual)		Token	Excess Return (%, Annual)		Carry (%, Annual)	
	Mean	Std.dev.	Mean	Std.dev.		Mean	Std.dev.	Mean	Std.dev.
1inch	2.67	17.52	2.02	4.38	kusama	20.71	25.96	13.99	0.84
aave	7.83	23.38	4.02	0.86	kyber	7.74	18.19	4.32	2.04
aion	8.76	16.37	5.57	0.48	livepeer	59.79	38.12	58.51	26.72
algorand	8.31	21.25	6.04	2.72	lto	10.65	18.69	6.80	0.85
ark	9.55	17.61	8.11	0.50	matic	32.26	40.29	23.53	12.09
avalanche	19.15	37.19	9.99	2.03	mina	13.63	22.56	11.75	0.28
band	15.37	25.93	12.70	1.51	mirror	40.07	36.68	43.10	24.83
bifi	10.12	20.00	7.95	3.57	near	18.59	23.51	11.50	1.20
binance-sc	13.50	15.18	11.33	3.31	nem	−1.88	13.54	−1.35	0.49
bitbay	18.36	77.83	1.06	0.74	neo	1.94	15.92	0.82	0.91
cardano	9.54	18.32	5.69	1.87	nuls	10.50	18.76	8.18	0.40
cosmos	12.30	19.99	8.91	1.48	oasis	18.97	25.39	15.25	2.31
cronos	6.98	14.82	8.18	0.40	pancakeswap	75.05	45.23	71.38	22.63
curve	5.49	21.52	3.03	1.86	peakdefi	43.78	37.06	43.09	17.31
dash	6.43	20.20	5.20	0.71	polkadot	16.07	20.28	11.90	1.39
decred	7.96	15.95	5.90	1.46	qtum	6.52	14.86	4.65	1.32
dfinity	9.26	16.95	14.49	2.32	secret	34.66	30.76	26.69	2.62
dodo	56.18	23.97	65.74	5.00	smartcash	4.05	18.53	1.62	0.28
elrond	26.07	30.28	17.44	7.12	snx	30.47	32.06	24.96	20.11
eos	4.72	16.53	4.39	3.94	solana	14.35	23.15	7.73	2.48
eth2.0	15.84	17.80	11.58	12.21	stafi	24.71	44.53	20.21	2.14
fantom	41.37	63.53	28.12	22.17	stake-dao	24.03	27.56	22.59	9.17
flow	4.49	14.05	9.21	0.71	sushi	8.75	19.58	10.38	4.47
harmony	18.14	28.10	10.31	0.79	tezos	6.96	17.90	5.38	0.82
icon	19.60	21.11	16.03	2.45	tron	5.65	16.08	3.36	1.69
idex	9.28	24.32	5.88	6.18	wanchain	10.30	16.13	7.37	0.30
injective	1.63	14.44	4.00	0.36	waves	7.21	20.22	3.96	1.70
iotex	10.85	22.54	8.50	2.70	wax	7.23	21.98	2.80	2.06
irisnet	15.33	23.31	9.64	0.39	yearn	9.55	30.27	4.68	2.79
kava	22.63	27.97	18.93	20.06	zcoin	18.18	25.12	14.87	3.53
US Dollar	0.00	0.00	0.00	0.00					

a week.

The performance of such crypto carry trade mainly measures the cross-sectional effect. Since we long high carry and short low carry, the portfolio carry is always positive. If the portfolio always achieves positive returns, it means that in the cross-section, assets with higher carry have greater aggregate returns.

The red curve in Figure 5 plots the cumulative return of such carry trade strategy. It shows an overall increase and large cumulative returns. Especially, in the cryptocurrency market where price volatility is huge, such a strategy performs a relatively smooth growth, implying the carry premia always exists. For further discussion, we also report two related strategies. The grey line shows the performance of the same carry portfolio but without

staking. That is, for long tokens, we do not stake them, and for the short assets, we also do not compensate for the staking reward rate. The strategy also exhibits increasing cumulative returns, which implies that the carry strategy earns excess returns not only from carry (staking reward) but also from price appreciation. Moreover, the blue line reports the performance of the same carry portfolio but is rebalanced every month. It exhibits less returns than 1W-carry trade. There are two potential explanations. First, as we discussed in our model, the reward rate will decrease with the staking ratio mechanically. Therefore, investors are unable to earn high carry consistently for a long period without timely position adjustments. Second, the reversal of reward rate further influences the staking ratio, which then weakens the effect on price appreciation as Table 4 reports.

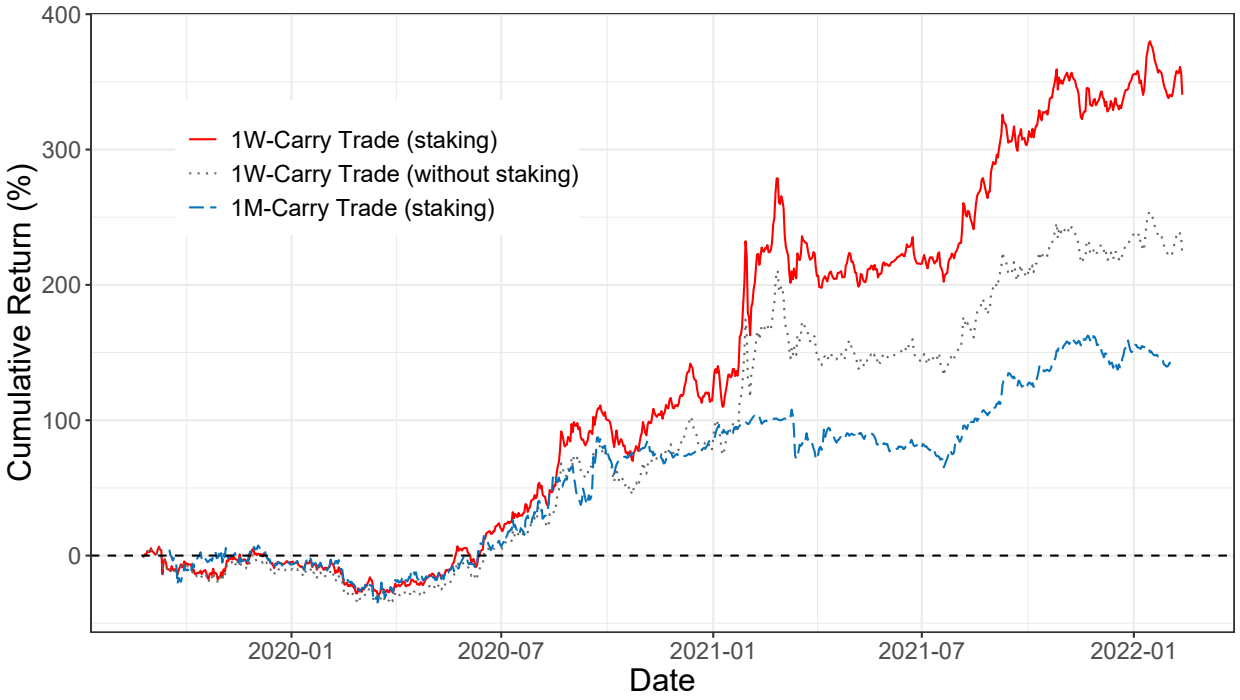

Figure 5: Cumulative returns of long-short carry trade strategies.
This figure shows the cumulative return of long-short carry strategies. The red line is the benchmark strategy. Tokens in the asset pool are ordered by their carry in the previous period. We go long the top $x\%$ high carry tokens with equal weight and short the bottom $x\%$ tokens with equal weight. For long tokens, we also stake them to earn the staking reward rate, while for the short assets, we also compensate for the staking reward rate. The portfolio is rebalanced every week. The choice of x does not affect our observation of the main characteristics. Here we set $x = 50$. Based on the benchmark strategy, the grey curve reports the performance of the strategy without earning or compensating staking rewards, the blue curve shows the performance of the strategy rebalanced every month.

The first row in Table 7 reports statics of the 1-Week carry strategy, including the

Table 7: Statistics of carry strategies.
This table reports the statistics of three strategies. The first row reports the results of the long-short carry strategy, which is corresponding to the red curve in Figure 5, The rows below report long strategies, including equal-weighted benchmark, the strategy that long only top 50% high carry tokens with equal weight, and the strategy that long only top 50% low carry tokens with equal weight. For each strategy, the annualized mean, standard deviations, skewness, kurtosis, maximum drawdown (MDD) and Sharpe ratio are reported.

Strategy	Mean (Annual, %)	St.dev. (Annual, %)	Skewness	Kurtosis	MDD (%)	Sharpe Ratio (Annual)
Long-short Strategy:						
1W-Carry Trade	69.23	42.98	−0.17	6.80	29.02	1.61
Long Strategy:						
EW	95.80	46.08	−1.14	6.76	32.88	2.08
EW High carry	139.32	54.16	−0.68	6.16	21.38	2.57
EW Low carry	70.08	47.67	−0.52	4.88	38.51	1.47

annualized mean, standard deviations, skewness, kurtosis, maximum drawdown and the Sharpe ratio. The results show that the carry strategy has a significantly greater positive return and yields a Sharpe ratio of 1.61. Examining the higher moments of the crypto carry trade return, we find that the strong negative skewness is associated with the currency carry trade shown by Brunnermeier et al. (2008). Moreover, the carry strategy exhibits excess kurtosis, indicating fat-tailed positive and negative returns, which is consistent with Koijen et al. (2018)'s findings for currencies and commodities.

We also report the statistics for the equal-weighted strategy in Table 7, i.e., borrow US dollars and go long all tokens in our sample with equal weight. Since the cryptocurrency market is generally in a bull market from 2019 to 2021, the equal-weighted benchmark earns extremely high beta returns and therefore has a very high Sharpe ratio of 2.08, while the carry strategy is a long-short strategy and does not earn market returns. As a comparison, we test the strategy that borrows US dollars and buys top 50% high carry tokens with equal weight. The order of the tokens is evaluated every week. Such a strategy outperforms the simple equal-weighted portfolio with a Sharpe ratio of 2.57. Figure 6 plots the cumulative returns of these two strategies. On the other hand, the strategy that goes long the 50% tokens with the lowest carry only yields a Sharpe ratio of 1.47. The comparisons also illustrate the positive correlation of carry to excess returns.

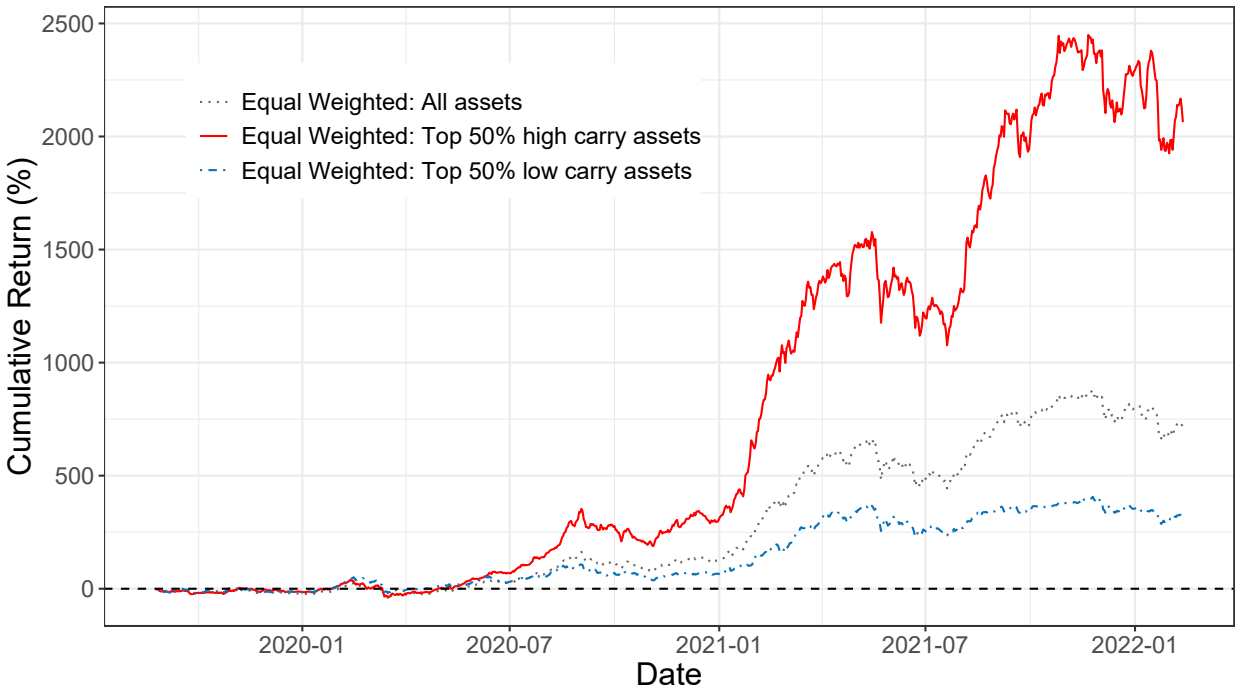

Figure 6: Cumulative returns of long strategies.
This figure shows the cumulative returns of the following two strategies. The grey curve corresponds to the equal-weighted benchmark, i.e., borrow US dollar and long all the tokens with equal weight. The red curve shows the result of the top 50% EW strategy, i.e., borrow US dollar and go long top 50% high carry tokens with equal weight. The blue curve shows the result of the lowest 50% EW strategy, i.e., borrow US dollar and go long the 50% tokens with the lowest carry with equal weight. The order of the tokens is evaluated every week.

6.3 Excess Return Predicted by Carry

Table 7 suggests that carry is a unique predictor of return. Considering (34), the predictability may be from two sources: the crypto carry itself, and any price appreciation that is related to or predicted by carry. To better understand the relationship between carry and expected returns, we follow Koijen et al. (2018) to run the following panel regression:

$$Excess\ Return\ _{i,t+1} = a_i + b_t + cCarry_{i,t} + \epsilon_{i,t}, \tag{40}$$

where a_i and b_t are crypto and time fixed effect respectively. By (34), $c = 0$ means the total return is unpredictable, while $c = 1$ suggests that expected return moves one-for-one with carry. If $c \in (0, 1)$, it implies that the market takes back part of the carry, i.e., investors cannot fully earn carry as their return.

Table 8 reports the results with and without fixed effects. Weekly and 14-day data are both used for robustness. Without token specific and time fixed effects, c represents the total predictability of returns from carry from both its passive and dynamic components. Token-specific fixed effects will remove the predictable return component of carry coming from passive exposure to tokens with different unconditional average returns.

The results in Table 8 imply that carry is a strong predictor of expected return. In Columns (1) and (3), without crypto specific fixed effect, the estimated coefficient is around 1, which means that high staking reward rate tokens neither depreciate nor appreciate on average. Hence, investors can earn reward rate differential using carry trade strategy. This is similar to the relevant findings for currency (Fama, 1984; Koijen et al., 2018).

Note that once token-specific effect is fixed, as Columns (2) and (4) in Panel B show, the estimated c is significantly positive but less than 1. This implies the market takes back a fraction of carry. In other words, time series carry predicts less expected return. According to Koijen et al. (2018), this is also found in commodities. When a commodity has a high spot price relative to its futures price, implying a high carry, the spot price tends to depreciate on average, thus lowering the realized return on average below the carry. For crypto in the staking economy, however, a different mechanism may be responsible for this phenomenon.

Table 8: Carry and excess returns

This table reports the results from the panel regression of (40), estimated c and t-statistics are reported. Without token-specific and time fixed effects, c represents the total predictability of returns from carry from both its passive and dynamic components. Including crypto specific fixed effects will remove the predictable return component of carry coming from passive exposure to tokens with different unconditional average returns. t-Statistics are reported in parentheses. ***,**,* indicate statistical significance at the 1%, 5% and 10% respectively.

Panel A: 7-day	$\text{ExcessReturn}_{i,t}$			
	(1)	(2)	(3)	(4)
$\text{Carry}_{i,t-1}$	0.987***	0.957***	1.005***	0.994***
	(37.675)	(20.331)	(45.059)	(24.140)
Fixed Effects				
Token		Y		Y
Time			Y	Y
Observations	3,927	3,927	3,927	3,927
R^2	0.266	0.097	0.352	0.137
Panel B: 30-day	$\text{ExcessReturn}_{i,t}$			
	(1)	(2)	(3)	(4)
$\text{Carry}_{i,t-1}$	1.022***	0.622**	1.073***	0.680***
	(6.926)	(2.349)	(8.392)	(2.888)
Fixed Effects				
Token		Y		Y
Time			Y	Y
Observations	902	902	902	902
R^2	0.051	0.007	0.076	0.010

In our model, while a high reward rate leads to a high staking ratio and thus a higher price appreciation, there is a downward adjustment effect of the reward rate in the time series. As the sum of carry (approximately equal to reward rate) and price appreciation, the excess return is then influenced by the adjustment. Comparing the results of weekly data with those of 30-day data, the downward adjustment effect is also magnified when the time window becomes larger, and thus the estimated c decreases in Columns (2) and (4) of Panel B. This also explains why there is such a difference in the results with and without fixed cross-sectional effects. In the case of commodity, the estimate of c is significantly smaller than 0 regardless of the fixed effect.

Overall, crypto carry exhibits characteristics partly similar to currencies and partly similar to commodities, rationalized by the mechanism of staking itself.

7 Conclusion

In addition to offering a convenience yield for transactions in digital networks, tokens are frequently staked (and slashed) for base-layer consensus generation or for incentivizing economic activities in DeFi protocols and platform development, and consequently earn stakers rewards akin to deposit interests. To analyze the economics of staking, we build the first dynamic model of a token-based economy where agents endogenously allocate wealth on and off a digital platform and use tokens either to earn rewards or to transact. We solve the mean field game with stochastic controls and systematic shocks, and identify staking ratio as a fundamental variable linking staking to the endogenous reward rate and token price.

The model rationalizes violations of the uncovered interest rate parity and significant crypto carry premia that we empirically document. For example, a strategy of buying high carry tokens and shorting low carry tokens yields a Sharpe ratio of 1.6, which can be attributed to transaction convenience in certain digital networks. We relate cryptocurrencies to other major asset classes such as currencies and commodities and verify model implications in the data. In particular, the staking ratio resembles liquidity and market depth since a high staking ratio leads to a lower amount of available tokens available for trade. Furthermore, the staking ratio is proportional to the reward rates in the cross-section but negatively correlated to reward rates in the time series; it positively predicts the returns of cryptocurrencies.

The framework can be further used to understand utilities of platform tokens. For example, DeFi projects increasingly lock up both native and non-native tokens. Allowing multiple tokens to be used within a network may cause the payment utility of native tokens to decline. But stable tokens entitle the holders to instead collect rewards (fees and subsidies), while providing functionalities such as security or liquidity for the networks. Optimally designing the various utilities of platform tokens and understanding their implications on token prices constitute interesting future research. Similarly, it remains an open question how staking and transaction interact in protocols with multiple types of tokens.

References

Abadi, Joseph and Markus Brunnermeier, "Blockchain economics," Technical Report, National Bureau of Economic Research 2018.

Achdou, Yves, Jiequn Han, Jean-Michel Lasry, Pierre-Louis Lions, and Benjamin Moll, "Income and wealth distribution in macroeconomics: A continuous-time approach," *The review of economic studies*, 2022, *89* (1), 45–86.

Backus, David K, Allan W Gregory, and Chris I Telmer, "Accounting for forward rates in markets for foreign currency," *The Journal of Finance*, 1993, *48* (5), 1887–1908.

Bailey, Warren and Kalok C Chan, "Macroeconomic influences and the variability of the commodity futures basis," *The Journal of Finance*, 1993, *48* (2), 555–573.

Bakshi, Gurdip and George Panayotov, "Predictability of currency carry trades and asset pricing implications," *Journal of financial economics*, 2013, *110* (1), 139–163.

Bansal, Ravi, "An exploration of the forward premium puzzle in currency markets," *The Review of Financial Studies*, 1997, *10* (2), 369–403.

_ and Wilbur John Coleman, "A monetary explanation of the equity premium, term premium, and risk-free rate puzzles," *Journal of Political Economy*, 1996, *104* (6), 1135–1171.

Barr, David G and Richard Priestley, "Expected returns, risk and the integration of international bond markets," *Journal of International money and finance*, 2004, *23* (1), 71–97.

Basu, Soumya, David Easley, Maureen O'Hara, and Emin Sirer, "StableFees: A Predictable Fee Market for Cryptocurrencie," *Available at SSRN 3318327*, 2019.

Bech, Morten L and Rodney Garratt, "Central bank cryptocurrencies," *BIS Quarterly Review September*, 2017.

Bekaert, Geert, "The time variation of risk and return in foreign exchange markets: A general equilibrium perspective," *The Review of Financial Studies*, 1996, *9* (2), 427–470.

Benhaim, Alon, Brett Hemenway Falk, and Gerry Tsoukalas, "Scaling Blockchains: Can Elected Committees Help?," *arXiv preprint arXiv:2110.08673*, 2021.

Bertucci, Charles, "Monotone solutions for mean field games master equations: continuous state space and common noise," *arXiv preprint arXiv:2107.09531*, 2021.

Biais, Bruno, Christophe Bisiere, Matthieu Bouvard, and Catherine Casamatta, "The blockchain folk theorem," *Review of Financial Studies*, 2019, *32* (5), 1662–1715.

_ , _ , _ , _ , and Albert J Menkveld, "Equilibrium bitcoin pricing," *Available at SSRN 3261063*, 2020.

Brunnermeier, Markus K and Yuliy Sannikov, "On the optimal inflation rate," *American Economic Review*, 2016, *106* (5), 484–89.

__ , **Stefan Nagel, and Lasse H Pedersen**, "Carry trades and currency crashes," *NBER macroeconomics annual*, 2008, *23* (1), 313–348.

Burnside, Craig, Martin Eichenbaum, Isaac Kleshchelski, and Sergio Rebelo, "Do peso problems explain the returns to the carry trade?," *The Review of Financial Studies*, 2011, *24* (3), 853–891.

Capponi, Agostino and Ruizhe Jia, "The Adoption of Blockchain-based Decentralized Exchanges: A Market Microstructure Analysis of the Automated Market Maker," *Available at SSRN 3805095*, 2021.

Cardaliaguet, Pierre, "Notes on mean field games," Technical Report, Technical report 2010.

__ **and Charles-Albert Lehalle**, "Mean field game of controls and an application to trade crowding," *Mathematics and Financial Economics*, 2018, *12* (3), 335–363.

__ **and Panagiotis Souganidis**, "On first order mean field game systems with a common noise," *arXiv preprint arXiv:2009.12134*, 2020.

__ **and** __ , "Weak solutions of the master equation for Mean Field Games with no idiosyncratic noise," *arXiv preprint arXiv:2109.14911*, 2021.

__ , **François Delarue, Jean-Michel Lasry, and Pierre-Louis Lions**, *The master equation and the convergence problem in mean field games*, Princeton University Press, 2019.

Carmona, Rene, "Applications of mean field games in financial engineering and economic theory," *arXiv preprint arXiv:2012.05237*, 2020.

Casassus, Jaime and Pierre Collin-Dufresne, "Stochastic convenience yield implied from commodity futures and interest rates," *The Journal of Finance*, 2005, *60* (5), 2283–2331.

Chiu, Jonathan, Seyed Mohammadreza Davoodalhosseini, Janet Hua Jiang, and Yu Zhu, "Bank market power and central bank digital currency: Theory and quantitative assessment," *Available at SSRN 3331135*, 2019.

Cong, Lin William and Simon Mayer, "The Coming Battle of Digital Currencies," *Available at SSRN 3992815*, 2021.

__ **and Yizhou Xiao**, "Categories and functions of crypto-tokens," in "The Palgrave Handbook of FinTech and Blockchain," Springer, 2021, pp. 267–284.

__ **and Zhiguo He**, "Blockchain disruption and smart contracts," *Review of Financial Studies*, 2019, *32* (5), 1754–1797.

__ , **George Andrew Karolyi, Ke Tang, and Weiyi Zhao**, "Value Premium, Network Adoption, and Factor Pricing of Crypto Assets," *Network Adoption, and Factor Pricing of Crypto Assets (December 2021)*, 2021.

__ , **Wayne R Landsman, Edward L Maydew, and Daniel Rabetti**, "Tax-Loss Harvesting with Cryptocurrencies," *Available at SSRN 4033617.*

_ , **Xi Li, Ke Tang, and Yang Yang**, "Crypto wash trading," *arXiv preprint arXiv:2108.10984*, 2021.

_ , **Ye Li, and Neng Wang**, "Token-based platform finance," *Journal of Financial Economics*, 2021.

_ , _ , **and** _ , "Tokenomics: Dynamic adoption and valuation," *Review of Financial Studies*, 2021, *34* (3), 1105–1155.

_ , **Zhiguo He, and Jiasun Li**, "Decentralized mining in centralized pools," *Review of Financial Studies*, 2021, *34* (3), 1191–1235.

Daniel, Kent, Robert Hodrick, and Zhongjin Lu, "The Carry Trade: Risks and Drawdowns," *Critical Finance Review*, 2017, *6* (2), 211–262.

Easley, David, Maureen O'Hara, and Soumya Basu, "From mining to markets: The evolution of bitcoin transaction fees," *Journal of Financial Economics*, 2019, *134* (1), 91–109.

Engel, Charles, "The forward discount anomaly and the risk premium: A survey of recent evidence," *Journal of empirical finance*, 1996, *3* (2), 123–192.

_ , "Exchange rates, interest rates, and the risk premium," *American Economic Review*, 2016, *106* (2), 436–74.

Fama, Eugene F, "Forward and spot exchange rates," *Journal of monetary economics*, 1984, *14* (3), 319–338.

_ **and Kenneth R French**, "Value versus growth: The international evidence," *The journal of finance*, 1998, *53* (6), 1975–1999.

Fanti, Giulia, Leonid Kogan, and Pramod Viswanath, "Economics of proof-of-stake payment systems," in "Working paper" 2019.

Feenstra, Robert C, "Functional equivalence between liquidity costs and the utility of money," *Journal of Monetary Economics*, 1986, *17* (2), 271–291.

Franz, Friedrich-Carl and Alexander Valentin, "Crypto Covered Interest Parity Deviations," *Available at SSRN 3702212*, 2020.

Gabaix, Xavier and Matteo Maggiori, "International liquidity and exchange rate dynamics," *The Quarterly Journal of Economics*, 2015, *130* (3), 1369–1420.

Gans, Joshua S, Hanna Halaburda et al., "Some economics of private digital currency," *Economic analysis of the digital economy*, 2015, pp. 257–276.

Griffin, John M and Amin Shams, "Is Bitcoin really untethered?," *Journal of Finance*, 2020, *75* (4), 1913–1964.

_ , **Xiuqing Ji, and J Spencer Martin**, "Momentum investing and business cycle risk: Evidence from pole to pole," *The Journal of finance*, 2003, *58* (6), 2515–2547.

Harvey, Campbell R, Ashwin Ramachandran, and Joey Santoro, *DeFi and the Future of Finance*, John Wiley & Sons, 2021.

Hinzen, Franz J, Kose John, and Fahad Saleh, "Proof-of-work's limited adoption problem," *NYU Stern School of Business*, 2019.

Hou, Kewei, G Andrew Karolyi, and Bong-Chan Kho, "What factors drive global stock returns?," *The Review of Financial Studies*, 2011, *24* (8), 2527–2574.

Howell, Sabrina T, Marina Niessner, and David Yermack, "Initial coin offerings: Financing growth with cryptocurrency token sales," *Review of Financial Studies*, 2020, *33* (9), 3925–3974.

Huang, Minyi, "Large-population LQG games involving a major player: the Nash certainty equivalence principle," *SIAM Journal on Control and Optimization*, 2010, *48* (5), 3318–3353.

Huberman, Gur, Jacob D Leshno, and Ciamac Moallemi, "Monopoly without a monopolist: An economic analysis of the bitcoin payment system," *Review of Economic Studies*, 2021, *88* (6), 3011–3040.

Ilmanen, Antti, "Time-varying expected returns in international bond markets," *The Journal of Finance*, 1995, *50* (2), 481–506.

Irresberger, Felix, Kose John, Peter Mueller, and Fahad Saleh, "The public blockchain ecosystem: An empirical analysis," *NYU Stern School of Business*, 2021.

Jiang, Zhengyang, Arvind Krishnamurthy, and Hanno Lustig, "Foreign safe asset demand and the dollar exchange rate," *The Journal of Finance*, 2021, *76* (3), 1049–1089.

John, Kose, Thomas J Rivera, and Fahad Saleh, "Economic implications of scaling blockchains: Why the consensus protocol matters," *Available at SSRN 3750467*, 2020.

_ , _ , and _ , "Equilibrium staking levels in a proof-of-stake blockchain," *Available at SSRN 3965599*, 2022.

Koijen, Ralph SJ, Tobias J Moskowitz, Lasse Heje Pedersen, and Evert B Vrugt, "Carry," *Journal of Financial Economics*, 2018, *127* (2), 197–225.

Krusell, Per and Anthony A Smith Jr, "Income and wealth heterogeneity in the macroeconomy," *Journal of political Economy*, 1998, *106* (5), 867–896.

Lasry, Jean-Michel and Pierre-Louis Lions, "Mean field games," *Japanese journal of mathematics*, 2007, *2* (1), 229–260.

Lehar, Alfred and Christine A Parlour, "Miner collusion and the bitcoin protocol," *Available at SSRN 3559894*, 2020.

Li, Tao, Donghwa Shin, and Baolian Wang, "Cryptocurrency pump-and-dump schemes," *Available at SSRN 3267041*, 2021.

Li, Zongxi, A Max Reppen, and Ronnie Sircar, "A mean field games model for cryptocurrency mining," *arXiv preprint arXiv:1912.01952*, 2019.

Lions, Pierre-Louis, "Courses at the Collège de France.," 2011.

Liu, Yukun, Aleh Tsyvinski, and Xi Wu, "Common risk factors in cryptocurrency," Technical Report, National Bureau of Economic Research 2019.

Lustig, Hanno, Andreas Stathopoulos, and Adrien Verdelhan, "The term structure of currency carry trade risk premia," *American Economic Review*, 2019, *109* (12), 4142–77.

_ , Nikolai Roussanov, and Adrien Verdelhan, "Common risk factors in currency markets," *The Review of Financial Studies*, 2011, *24* (11), 3731–3777.

_ , _ , and _ , "Countercyclical currency risk premia," *Journal of Financial Economics*, 2014, *111* (3), 527–553.

Lyandres, Evgeny, Berardino Palazzo, and Daniel Rabetti, "Do tokens behave like securities? An anatomy of initial coin offerings," *SSRN Electronic Journal*, 2019.

Makarov, Igor and Antoinette Schoar, "Trading and arbitrage in cryptocurrency markets," *Journal of Financial Economics*, 2020, *135* (2), 293–319.

Menkhoff, Lukas, Lucio Sarno, Maik Schmeling, and Andreas Schrimpf, "Carry trades and global foreign exchange volatility," *The Journal of Finance*, 2012, *67* (2), 681–718.

Prat, Julien, Vincent Danos, and Stefania Marcassa, "Fundamental pricing of utility tokens," 2019.

Rudin, Walter et al., *Principles of mathematical analysis*, Vol. 3, McGraw-hill New York, 1964.

Saleh, Fahad, "Blockchain without waste: Proof-of-stake," *Review of Financial Studies*, 2021, *34* (3), 1156–1190.

Tang, Ke and Haoxiang Zhu, "Commodities as collateral," *The Review of Financial Studies*, 2016, *29* (8), 2110–2160.

_ and Wei Xiong, "Index investment and the financialization of commodities," *Financial Analysts Journal*, 2012, *68* (6), 54–74.

Valchev, Rosen, "Bond convenience yields and exchange rate dynamics," *American Economic Journal: Macroeconomics*, 2020, *12* (2), 124–66.

Verdelhan, Adrien, "A habit-based explanation of the exchange rate risk premium," *The Journal of Finance*, 2010, *65* (1), 123–146.

Yong, Jiongmin and Xun Yu Zhou, *Stochastic controls: Hamiltonian systems and HJB equations*, Vol. 43, Springer Science & Business Media, 1999.

Appendix

A. Proofs for Propositions

A.1 Derivation of the Master Equation

The relationship between the MFGs and the master equation. We first briefly explain the relationship between the classical MFG system (a couple of PDEs) and the master equation based on our model as an example. The more detailed discussions are provided in Cardaliaguet et al. (2019). We now consider the evolution of the mean field of this framework, i.e., the distribution of investors' wealth $m_t(w_t)$. In our model, there is no idiosyncratic shock to agents. They suffer a systematic shock by token price with heterogeneous exposure. Recall the wealth dynamic of each agent as (10) shows, in which Z_t stands for a systematic shock. Such shock impacts all the agents and thus causes m_t to be a flow of measures (Cardaliaguet et al., 2019), and precisely, the flow of conditional marginal measures of agents' wealth given the realization of Z_t. The dynamic of m_t is then characterized by the stochastic Fokker-Planck equation (A.1), with initial condition $m_0(w_t) = m_0$.

$$
\begin{aligned}
\mathrm{d}_t m_t = & \left[-\frac{\partial}{\partial w}\left(m_t \frac{\partial H}{\partial \xi}(w, \frac{\partial J}{\partial w}, \frac{\partial^2 J}{\partial w^2}; m_t, r, A_t) \right) + \frac{\partial^2}{\partial w^2}\left(m_t \frac{\partial H}{\partial \zeta}(w, \frac{\partial J}{\partial w}, \frac{\partial^2 J}{\partial w^2}; m_t, r, A_t) \right) \right] \mathrm{d}t \\
& - \frac{\partial}{\partial w}\left(m_t \sqrt{2 \frac{\partial H}{\partial \zeta}(w, \frac{\partial J}{\partial w}, \frac{\partial^2 J}{\partial w^2}; m_t, r, A_t)} \mathrm{d}Z_t \right) \\
= & \left[-\frac{\partial}{\partial w}\left(f^*(w; m_t, r, A_t) m_t \right) + \frac{1}{2}\frac{\partial^2}{\partial w^2}\left(g^*(w; m_t, r, A_t)^2 m_t \right) \right] \mathrm{d}t \\
& - \frac{\partial}{\partial w}\left(g^*(w; m_t, r, A_t) m_t \mathrm{d}Z_t \right),
\end{aligned}
\tag{A.1}
$$

where $f^*(w; m_t, r, A_t)$ and $g^*(w; m_t, r, A_t)$ are the corresponding values of f and g when $\{y, x, l\}$ satisfies the maximum principle, respectively. The corresponding HJB equation (12) is also rendered to be a stochastic PDE since it is related to m. By now, we obtain a pair of coupled PDEs with unknowns $\{J, m\}$ as we do in the classical MFG framework. The difference is that the PDEs here are stochastic. As we discussed in the main text in Section 3.3, the value function of the master equation, U can be considered as a advanced version of J, which involves the potential impact of m. Precisely, let $\{J, m\}$ be a solution of the coupled PDEs, and U be a solution of the master

equation, we have

$$\begin{aligned}
\mathrm{d}_t m_t = &\left[-\frac{\partial}{\partial w}\left(m_t \frac{\partial H}{\partial \xi}(w, \frac{\partial U}{\partial w}, \frac{\partial^2 U}{\partial w^2}; m_t, r, A_t)\right) + \frac{\partial^2}{\partial w^2}\left(m_t \frac{\partial H}{\partial \zeta}(w, \frac{\partial U}{\partial w}, \frac{\partial^2 U}{\partial w^2}; m_t, r, A_t)\right)\right]\mathrm{d}t \\
&- \frac{\partial}{\partial w}\left(m_t \sqrt{2\frac{\partial H}{\partial \zeta}(w, \frac{\partial U}{\partial w}, \frac{\partial^2 U}{\partial w^2}; m_t, r, A_t)}\mathrm{d}Z_t\right), \\
&J_t(w_t; m_t, r, A_t) = U(w_t, m_t, A_t), \qquad t \in [0, \infty), a.s..
\end{aligned} \tag{A.2}$$

Relevant definitions and requirements. We first introduce the following definitions and notations. The set $\mathcal{P}(\mathbb{R})$ of measures on $\mathbb{R}$ is endowed with the Monge-Kantorovich distance,

$$\mathbf{d}(m, m') = \sup_{\Xi} \int_{\mathbb{R}} \Xi(y)\mathrm{d}(m - m')(y), \tag{A.3}$$

where the supremum is taken over all Lipschitz continuous maps $\Xi : \mathbb{R} \mapsto \mathbb{R}$ with a Lipschitz constant bound by 1.[33] As Eq.(19) shows, the master equation involves derivatives of the unknown with respect to the measure m. The formal definitions are provided below, which also follow Cardaliaguet et al. (2019).

Definition 1. *We say that $U : \mathcal{P}(\mathbb{R}) \to \mathbb{R}$ is $\mathcal{C}^1$, if there is a continuous map $\frac{\delta U}{\delta m} : \mathcal{P}(\mathbb{R}) \times \mathbb{R} \to \mathbb{R}$ such that, for any $m, m' \in \mathcal{P}(\mathbb{R})$,*

$$\lim_{s \to 0^+} \frac{U((1-s)m + sm') - U(m)}{s} = \int_{\mathbb{R}} \frac{\delta U}{\delta m}(m, y)\mathrm{d}(m' - m)(y). \tag{A.4}$$

Definition 2. *We say that $U : \mathcal{P}(\mathbb{R}) \to \mathbb{R}$ is $\mathcal{C}^2$, if for a fixed $y \in \mathbb{R}$, the map $m \mapsto \frac{\delta U}{\delta m}(m, y)$ is $\mathcal{C}^1$. Moreover, denote its derivative as $\frac{\delta^2 U}{\delta m^2} : \mathcal{P}(\mathbb{R}) \times \mathbb{R} \times \mathbb{R} \to \mathbb{R}$. It satisfies*

$$\frac{\delta U}{\delta m}(m', y) - \frac{\delta U}{\delta m}(m, y) = \int_0^1 \int_{\mathbb{R}} \frac{\delta^2 U}{\delta m^2}\Big((1-s)m + sm', y, y'\Big)\mathrm{d}(m' - m)y'\mathrm{d}s \tag{A.5}$$

To derive the master equation, we need the additional assumptions on the mathematical properties of $U(w, m, A)$ to make the terms in (19) well defined. Precisely, U is continuous in all its arguments (especially, for the $\mathbf{d}$ distance on $\mathcal{P}(\mathbb{R})$ for the measure m), is of class $\mathcal{C}^2$ in w, A and m. Especially for m, the first and second order derivatives, $\frac{\delta U}{\delta m}(w, m, A, y)$ and $\frac{\delta^2 U}{\delta m^2}(w, m, A, y, y')$, are continuous in all the arguments. $\frac{\delta U}{\delta m}(w, m, A, y)$ is twice differentiable in y. $\frac{\delta^2 U}{\delta m^2}(w, m, A, y, y')$ is

[33] As the online Appendix of Achdou et al. (2022) also discusses, in the theoretical literatures, the space is often specified as the n-dimensional torus $\mathbb{T}^n$ rather than $\mathbb{R}^n$. The only reason is to sidestep the discussion of boundary conditions in the space dimension.

twice differentiable in (y, y'). The derivatives are continuous in all the arguments. These requirements are not difficult to satisfy under the usual settings of utilities, initial measures, etc..

Derive the master equation. We start with the time-dependent case first, where the value function of the master equation, U, can be represented as $U = U(t, w, m, A)$, while the value function in the HJB equation, $J(t, w, A; m, r)$, in which $\{m, r\}$ is considered as given parameters as discussed in Section 3.3. Note that in Section 3.2, we are solving a simple case that m is determined or satisfies a deterministic evolution process (i.e., the Fokker-Planck equation in the classical MFG system. Appendix C. provides more detailed descriptions on MFG.). However, in the MFGs with systematic shock, the FP equation that m satisfies becomes stochastic as is shown in (A.1), which also renders the value function J to be random. Denote the random value function as $\tilde{J}(t, w, A_t)$. Given the initial distribution m_{t_0} and the initial productivity A_{t_0} at $t_0 = 0$, we have

$$\tilde{J}(t_0, w, A_{t_0}) = J(t_0, w, A_{t_0}; m_{t_0}, r_{t_0}) = U(t_0, w, m_{t_0}, A_{t_0}). \tag{A.6}$$

As time t changes, the system becomes stochastic. By the Lemma 5.1 in Cardaliaguet et al. (2019), we construct a connection of the value functions of the HJB equation and the master equation.

$$\tilde{J}(t, w, A_t) = U(t, w + \int_0^t g^*(w, s)\mathrm{d}Z_s, m_{0,t}, A_t), \tag{A.7}$$

where $m_{0,t}$ is the image of $\tilde{m}_t$ by the random mapping, $w \mapsto w + \int_0^t g^*(w, s)\mathrm{d}Z_s$, $\tilde{m}_t(w) = m_t(w + g^*(w, t)Z_t)$. Then consider the case when we are at t_0, $t_0 \in (0, \infty)$, i.e. m_{t_0} is given,

$$\begin{aligned}
&\frac{U(t_0 + h, w, m_{t_0}, A_{t_0}) - U(t_0, w, m_{t_0}, A_{t_0})}{h} \\
=&\frac{\mathrm{E}_{t_0}\left[\tilde{J}(t_0 + h, w, A_{t_0+h})\right] - \tilde{J}(t_0, w, A_{t_0})}{h} + \frac{U(t_0 + h, w, m_{t_0}, A_{t_0}) - \mathrm{E}_{t_0}\left[\tilde{J}(t_0 + h, w, A_{t_0+h})\right]}{h}.
\end{aligned} \tag{A.8}$$

When $h \to 0$, the first term in the right-hand side of (A.8) satisfies

$$\begin{aligned}
&\lim_{h\to 0} \mathrm{E}_{t_0}\left[\tilde{J}(t_0 + h, w, A_{t_0+h})\right] - \tilde{J}(t_0, w, A_{t_0}) = \frac{\partial \tilde{J}}{\partial t}(t_0, w, A_{t_0}) \\
=& - H\bigg(w, \frac{\partial U}{\partial w}(w, m_{t_0}, A_{t_0}), \frac{\partial^2 U}{\partial w^2}(w, m_{t_0}, A_{t_0}); m_{t_0}, r_{t_0}, A_{t_0}\bigg) \\
&- \bigg(\mu^A A_{t_0}\frac{\partial U}{\partial A}(w, m_{t_0}, A_{t_0}) + \frac{1}{2}(\sigma^A A_{t_0})^2\frac{\partial^2 U}{\partial A^2}\bigg),
\end{aligned} \tag{A.9}$$

which has a similar deriving process and form to the HJB equation since the "stochastic" components has been omitted by the expectation. As for the second term, we need a specific form

of Itô's formula to deal with $\mathrm{d}_t U$, which is, fortunately, provided and proved in Lemma 5.15 of Cardaliaguet et al. (2019). We obtain

$$
\begin{aligned}
&\lim_{h\to 0}\frac{U(t_0+h,w,m_{t_0},A_{t_0})-\mathrm{E}_{t_0}\left[\tilde{J}(t_0+h,w,A_{t_0+h})\right]}{h}\\
=&\lim_{h\to 0^+}\frac{1}{h}\mathrm{E}_{t_0}\left[U(t_0+h,w,m_{t_0},A_{t_0})-U(t_0+h,w+\int_{t_0}^{t_0+h}g^*(w,s)\mathrm{d}Z_s,m_{t_0,t_0+h},A_{t_0+h})\right]\\
=&\int_{\mathbb{R}}\frac{\partial}{\partial y}\frac{\delta\hat{U}}{\delta m}(t_0,w,m_{t_0},A_{t_0},y)\mathrm{d}m_{t_0}(y)+2\int_{\mathbb{R}}\frac{\partial}{\partial w}\frac{\delta\hat{U}}{\delta m}(t_0,w,m_{t_0},A_{t_0},y)\mathrm{d}m_{t_0}(y)\\
&+\int_{\mathbb{R}\times\mathbb{R}}\frac{\partial^2}{\partial y\partial y'}\frac{\delta^2\hat{U}}{\delta m^2}(t_0,w,m_{t_0},A_{t_0},y,y')\mathrm{d}m_{t_0}(y)\mathrm{d}m_{t_0}(y')+\frac{\partial^2\hat{U}}{\partial w^2}(t_0,w,m_{t_0},A_{t_0})\\
&-\int_{\mathbb{R}}\frac{\delta U}{\delta m}(t_0,w,m_{t_0},A_{t_0},y)\cdot\frac{\partial H}{\partial\xi}\left(w,\frac{\partial U}{\partial w}(t_0,y,m_{t_0},A),\frac{\partial^2 U}{\partial w^2}(t_0,y,m_{t_0},A);m_{t_0},r_{t_0},A_{t_0}\right)\mathrm{d}m_{t_0}(y),
\end{aligned}
\tag{A.10}
$$

where $\hat{U}:[0,\infty)\times\mathbb{R}\times\mathcal{P}^2(\mathbb{R})\times\mathbb{R}\to\mathbb{R}$, $\hat{U}(t,w,m,A)=\frac{\partial H}{\partial\zeta}(w,\frac{\partial U}{\partial w},\frac{\partial^2 U}{\partial w^2};m,r,A)\cdot U(t,w,m,A)=\frac{1}{2}g^*(w,t)\cdot U(t,w,m,A)$. The second equal sign comes from Lemma 5.15 of Cardaliaguet et al. (2019). We have two differences here. First, in the Lemma, the agent's sensitivity to the systematic shock is normalized to 1 for simplicity, whereas here we use g^*. Second, the *Hamilton* here has the opposite sign. There is no difficulty in applying the results with some modification.

Turn to (A.8). Let $h\to 0$ and substitute (A.9), (A.10). Note that the discount factor $e^{-\phi h}\approx 1-\phi h$ when h is close to zero, which allow us to do use $U(t_0+h,w,A_{t_0})\approx(1-\phi h)U(t_0,w,A_{t_0})$. Based on this common treatment, it is not difficult to transform the time-dependent equations into the time-independent case. We obtain a time-independent master equation (19):

$$
\begin{aligned}
\phi U(w,m,A)=&H\left(w,\frac{\partial U}{\partial w}(w,m,A),\frac{\partial^2 U}{\partial w^2}(w,m,A);m,r,A\right)\\
&+\int_{\mathbb{R}}\frac{\delta U}{\delta m}(w,m,A,y)\cdot\frac{\partial H}{\partial\xi}\left(w,\frac{\partial U}{\partial w}(y,m,A),\frac{\partial^2 U}{\partial w^2}(y,m,A);m,r,A\right)\mathrm{d}m(y)\\
&-\left[\int_{\mathbb{R}}\frac{\partial}{\partial y}\frac{\delta\hat{U}}{\delta m}(w,m,A,y)\mathrm{d}m(y)+2\int_{\mathbb{R}}\frac{\partial}{\partial w}\frac{\delta\hat{U}}{\delta m}(w,m,A,y)\mathrm{d}m(y)\right.\\
&\left.+\int_{\mathbb{R}\times\mathbb{R}}\frac{\partial^2}{\partial y\partial y'}\frac{\delta^2\hat{U}}{\delta m^2}(w,m,A,y,y')\mathrm{d}m(y)\mathrm{d}m(y')\right]-\frac{\partial^2\hat{U}}{\partial w^2}(w,m,A)\\
&-\left[\mu^A A\frac{\partial U}{\partial A}(w,m,A)+\frac{1}{2}(\sigma^A A)^2\frac{\partial^2 U}{\partial A^2}(w,m,A)\right].
\end{aligned}
\tag{A.11}
$$

The solution to the master equation. The classical solution to the second order master equation is, naturally, a map $U:\mathbb{R}\times\mathcal{P}(\mathbb{R})\times\mathbb{R}\mapsto\mathbb{R}$, which satisfies all the requirements in the relevant definition part in this section, and satisfies the master equation. In our framework, there is no idiosyncratic Brownian shock, which generates additional problem that the solution

may not be smooth. Fortunately, we can refer to the definition of the weak solution introduced by Cardaliaguet and Souganidis (2021) that focus on the master equation with no idiosyncratic shock. [34] The relationship between the weak solution and the classical solution is that if U^* is a weak solution, and U, $\frac{\partial U}{\partial w}$, $\frac{\delta U}{\delta m}$, $\frac{\partial^2 U}{\partial w^2}$, $\frac{\delta^2 U}{\delta m^2}$ and $\frac{\partial}{\partial w}\frac{\delta}{\delta m}U$ are continuous in w and m, then U^* is a classical solution of the master equation, U^{**}, up to adding a continuous function of m, $c^*(m)$, i.e.,

$$U^*(w, m, A) = U^{**}(w, m, A) + c^*(m). \tag{A.12}$$

It is because the definition of the weak solution actually characteristics $\frac{\partial U}{\partial w}$ and not U. Under proper assumptions, the existence and uniqueness of the weak solution have been proved. In the framework here, especially, the Larsy-Lions monotonicity condition naturally is easy to hold since we do not have the so-called coupled payoff terms[35] in agents' optimization problems.

A.2 Proof of Proposition 1

For each agent, she solves the optimization problem in the situation that $\{m, r\}$ is given. Consider the master equation,[36] the marginal utility of staked and non-staked tokens are

$$\begin{aligned} MU_l &= (\mu_t + r_t - c_t + \frac{\partial \Psi}{\partial n_t})\partial_w U + (x_t + l_t)\sigma_t^2 \partial_{ww} U, \\ MU_x &= \left(\mu_t + (1-\alpha)\left(\frac{A_t u_t}{x_t}\right)^{\alpha} + \frac{\partial \Psi}{\partial n_t}\right)\partial_w U + (x_t + l_t)\sigma_t^2 \partial_{ww} U. \end{aligned} \tag{A.13}$$

Note that MU_x and MU_l contains some common terms, including price appreciation μ, loss of numeraire convenience $-\frac{\partial \Psi}{\partial n_t}$ and volatility risk of token price. Agents will always obtain these part of utility once they hold tokens. Therefore, agents make choices between staking and non-staking by comparing the remaining terms, $(r_t - c_t)$ and $(1-\alpha)\left(\frac{A_t u_t}{x_t}\right)^{\alpha}$. The marginal return of staked token remains the same, while the marginal utility of non-staked token diminishes to zero. In addition, $x_t \to 0_+$, the marginal utility of non-staked token must exceed $r_t - c_t$. That is, there exists a unique $\tilde{x}_t$ that satisfies

$$r_t - c_t = (1-\alpha)\left(\frac{A_t u_t}{\tilde{x}_t}\right)^{\alpha}. \tag{A.14}$$

[34] The solution is solved by the Hilbert space approach introduced by Lions (2011), the detailed notion of the weak solution is provided in Cardaliaguet and Souganidis (2021). Here we no longer repeat existing work.

[35] Such term is often represented as $F(\cdot)$ in MFG papers.

[36] It is equivalent to consider the HJB equation when solving the optimization problem of one agent. The additional terms in the master equation does not directly involve the agent's controls as arguments. On the other hand, the agent have negligible impact on the distribution m.

The agent will first choose to keep enough tradable tokens for earning transaction convenience. Once her holding of non-staked tokens x_t reaches $\tilde{x}_t$, she will turn to stake the remaining tokens (if enough tokens are held). Combining with the wealth constraint, we obtain

$$\tilde{x}_t = \min\left\{w_t, \left(\frac{1-\alpha}{r_t - c_t}\right)^{\frac{1}{\alpha}} A_t u_t\right\}. \tag{A.15}$$

Note that agents will choose not to participate when the realized transaction convenience is non-positive. As (3) shows, once the agent participates, i.e. $x_t > 0$, the transaction utility flow increases with x_t. Therefore, $\tilde{x}_t$ will be realized if and only if $\tilde{x}_t^{1-\alpha}(A_t u_t)^{\alpha} - \varphi > 0$. We call this intermediate variable as necessary value of x_t, and denote it as $\hat{x}_t$. $\hat{x}_t$ satisfies

$$\hat{x}_t = \tilde{x}_t \cdot \mathbb{I}\left\{\tilde{x}_t > \left(\frac{\varphi}{(A_t u_t)^{\alpha}}\right)^{\frac{1}{1-\alpha}}\right\}, \tag{A.16}$$

where $\mathbb{I}$ is an indicator function.

$\hat{x}_t$ ensures participation and optimality compared to staking. On the other hand, let us consider the aggregate holding of tokens, $q_t = x_t + l_t$. The marginal utility of holding tokens should be the upper envelope of the marginal utility of the two holding ways. Based on the above discussion, we obtain

$$MU_q = \left(\mu_t + \max\left\{r_t - c_t, (1-\alpha)\left(\frac{A_t u_t}{q_t}\right)^{\alpha}\right\} + \frac{\partial \Psi}{\partial n_t}\right)\partial_w U + q_t \sigma_t^2 \partial_{ww} U. \tag{A.17}$$

MU_q decreases strictly with q_t (note that $\partial_w U > 0$ and $\partial_{ww} U < 0$). In addition, when $q_t \to 0_+$, the *max* term tends to positive infinity. Therefore, there exists and only exists the following two cases. First, there is a unique $q_t^* \leqslant w_t$ that satisfies the first order condition. Second, $MU_q(w_t) > 0$, then agent will allocate all her wealth into the platform. As a conclusion, the agent has a unique and positive optimal choice q_t^*.

Then, we obtain $x^* = \min\{q_t^*, \hat{x}_t\}$.

Rearrange the expression of optimal individual staking ratio θ_t^*,

$$\theta_t^* = \frac{l_t^*}{q_t^*} = 1 - \frac{x_t^*}{q_t^*} = 1 - \frac{\min\{q_t^*, \hat{x}_t\}}{q_t^*}, \tag{A.18}$$

where the economic meaning of the minimized term is that when $x_t \leqslant \hat{x}_t$, earning transaction convenience is better than earning staking reward, while when $x_t \leqslant q_t^*$, holding tradable token is better than holding numeraire. Substituting (A.14) and (A.16) into (A.18), then Proposition 1 is proved.

Based on the above results, we have the following intuitions.

First, agents' individual staking ratios increase with reward rate r_t. Consider the impact of reward rate r_t. As r_t increases, the marginal utility of staked token increases, while both the convenience of token and numeraire remains the same. Intuitively, agents will increase the proportion of staking. Mathematically, an increase in r_t will cause the *max* term in (A.17) to increase (non-strictly), so that q_t^* increases. Substituting into (21), we obtain a larger optimal θ_t^*.

Second, agents have heterogeneous optimal staking choices, which are related to their wealth. Note that in the expression of θ_t^*, both u_t and q_t^* are relative to agent's wealth. Therefore, the optimal individual staking ratio may be different among agents due to the difference of wealth level. In numerical analysis, after we make more detailed assumptions on the user type u_t, We will examine the difference between the optimal decisions of agents with different wealth levels. Especially, when u_t increases monotonically in w_t with a diminishing marginal change, the agent who owns more wealth will decide to invest a greater proportion for staked tokens.

A.3 Proof of Proposition 2

We first analyse the resulting overall staking ratio under a given reward rate r_t, $\Theta(r_t)$. (Without causing misunderstanding, we omit m and A in the cross-sectional derivation.) Following the proof of Proposition 1, we obtain $x_t^* = \min\{q_t^*, \hat{x}_t\} = \min\left\{q_t^*, \tilde{x}_t \cdot \mathbb{I}\left\{\tilde{x}_t > \left(\frac{\varphi}{(A_t u_t)^\alpha}\right)^{\frac{1}{1-\alpha}}\right\}\right\}$.

First, consider the case that the indicator function equals one for all agents. Treat $\tilde{x}$ as a function of individual wealth w and global reward rate r at time t, $\tilde{x}_t$ is differentiable to r and $\frac{\partial \tilde{x}(w,r)}{\partial r} < 0$. On the other hand, when $x_t^* = q_t^*$, i.e. $q_t^* \leqslant \tilde{x}_t$, the *max* term in (A.17) equals to $(1-\alpha)\left(\frac{A_t u_t}{q_t}\right)^\alpha$. q_t^* solves the first order condition for any given r, thus q_t^* can be treated as a function of r that is shown to be differentiable, $\frac{\partial q_t^*(w,r)}{\partial r} \leqslant 0$.

Note that $\forall i$, $w_i \in W$, where $W \equiv [0, \overline{w}]$ is a closed set. We have obtained that $x^*(w,r)$ is differentiable with respect to r at r_j, $\forall w \in W \backslash W_j$, where W_j is defined as, $\forall w \in W_j$, $x^*(w, r_j) = q^*(w, r_j)$, and $\forall r' > r_j$, $x^*(w, r') = \tilde{x}(w, r')$. In fact, x^* may also be differentiable to r at r_j for $w \in W_j$. However, we do not need this stronger condition. Since U is monotonous in w, the measure of W_j is always zero for any r_j.

Consider the definition of overall staking ratio Θ as in (14), $\Theta(r)$ is differentiable and satisfies

$$
\begin{aligned}
\Theta'(r) &= \frac{\mathrm{d}}{\mathrm{d}r}\frac{\int_W l(w,r)m(w)\mathrm{d}w}{\int_W q(w,r)m(w)\mathrm{d}w} = \frac{(\frac{\mathrm{d}}{\mathrm{d}r}\int_{W\backslash W_r} lm\mathrm{d}w)(\int_W qm\mathrm{d}w) - (\int_W lm\mathrm{d}w)(\frac{\mathrm{d}}{\mathrm{d}r}\int_{W\backslash W_r} qm\mathrm{d}w)}{(\int_W qm\mathrm{d}w)^2} \\
&= \frac{(\int_{W\backslash W_r} \frac{\partial l(w,r)}{\partial r} m\mathrm{d}w)(\int_W qm\mathrm{d}w) - (\int_W lm\mathrm{d}w)(\int_{W\backslash W_r} \frac{\partial q(w,r)}{\partial r} m\mathrm{d}w)}{(\int_W qm\mathrm{d}w)^2} \\
&= \frac{(\int_{W\backslash W_r} \frac{\partial l}{\partial r} m\mathrm{d}w)(\int_W xm\mathrm{d}w) - (\int_W lm\mathrm{d}w)(\int_{W\backslash W_r} \frac{\partial x}{\partial r} m\mathrm{d}w)}{(\int_W qm\mathrm{d}w)^2} \geqslant 0,
\end{aligned}
\tag{A.19}
$$

where the third equal sign holds by Theorem 9.42 in Rudin et al. (1964). As for the case that $\exists\Omega \neq \varnothing$, s.t. $\forall w_t \in \Omega$, the indicator function equals zero. We define Ω_j as, $\forall w \in \Omega_j$, $\tilde{x}(w, r_j) = \left(\frac{\varphi}{(A_t u_t)^\alpha}\right)^{\frac{1}{1-\alpha}}$. By the monotonicity, $\forall r' > r_j$, $\tilde{x}(w, r') < \left(\frac{\varphi}{(A_t u_t)^\alpha}\right)^{\frac{1}{1-\alpha}}$, i.e. the indicator function equals zero. Note that the measure of $W\Omega_j$ is always zero for any r_j. The following proof process goes similarly to the above.

In equilibrium under given positive aggregate reward, ρ, reward rate and staking ratio should satisfy the fixed point equation in (15), i.e., $r\Theta(r) = \rho > 0$. Note the following properties: (i) $r\Theta(r)$ weakly increases in r, and especially, strictly increases in r for any positive $\Theta(r)$. (ii) $r\Theta(r) = 0$ when r equals zero. (iii) $\lim_{r\to+\infty} r\Theta(r) = r > \rho$. Therefore, $\forall\rho$, $0 < \rho < \infty$, there exists a unique r that satisfies the fixed point problem.

Now considering the case as Proposition 2 describes, $\forall\rho' > \rho > 0$, denote the resulting equilibrium reward rate as r' and r respectively. By the monotonicity of $r\Theta(r)$, we obtain $r' > r$. Then by (A.19), the resulting equilibrium staking ratio satisfies $\Theta(r') > \Theta(r)$, i.e., $\Theta(\rho') > \Theta(\rho)$.

A.4 Proof of Proposition 3

Since P_t can be separately represented as $P(A_t, Q_t) = \frac{1}{Q_t}V(A_t)$, we can analytically derive the partial differentials of P_t. Substituting the differentials into (27) and rearranging the equation, we obtain the ordinary differential equation for $V(A_t)$ as Eq.(30) shows.

Consider the lower boundary condition when $A_t \to 0$. Intuitively, when $A_t = 0$, the platform has no productivity and no agent participates. Therefore, the resulting token price must be zero. Specifically, by Eq.(A.15), $\tilde{x} \to 0$. Agents cannot realize positive transaction utility flow. That is, agents' individual staking ratio tends to 1.[37] Then the reward rate r_t is close to the reward ratio ρ_t, and $q_t \to l_t$, for any agents. Substituting into the F.O.C. of the HJB equation, we have

$$0 = \left(\mu_t + \rho_t - c_t + \frac{\partial\Psi_t}{\partial n_t}\right)\frac{\partial_w U}{\partial_{ww} U} + \sigma_t^2 q_t. \tag{A.20}$$

As mentioned in the maintext, we further assume that when $A_t \to 0$, $\forall y_t > 0$, Ψ_t is sufficiently large. This assumption captures the case that when the platform has almost zero productivity, the platform token is useless and the relative convenience of numeraire is therefore large. Specifically, we follow Bansal and Coleman (1996) and Valchev (2020) and define Ψ takes the following form:

$$\Psi_t = \Psi(y_t, n_t, A_t) = \bar{\psi}(A_t) y_t^{\beta} n_t^{1-\beta}, \tag{A.21}$$

[37] Here we focus on the case that the reward rate r_t is always larger than staking cost c_t no matter what the overall staking ratio is, i.e., $c_t < \rho_t = \min_{\Theta_t\in[0,1]} r(\rho_t, \Theta_t)$. Otherwise, staking is obviously a "bad" choice for agents.

where $\beta > 1$. To satisfy the assumption above, we let $\bar{\psi}'(A_t) < 0$, $\lim_{A_t \to 0} \bar{\psi}(A_t) = \infty$, and $\lim_{A_t \to \infty} \bar{\psi}(A_t) = 0$. Then, $\frac{\partial \Psi_t}{\partial n_t} = -(\beta - 1)\bar{\psi}(A_t)(\frac{y_t}{n_t})^{\beta}$. Under such sufficient condition, we obtain that as $A_t \to 0$, Eq.(A.20) is negative, $\forall q_t \geqslant 0$. Therefore, $\lim_{A_t \to 0} V(A_t) = 0$.

As for the upper boundary, the intuition is that all the wealth will be attracted to the platform when A_t is sufficiently high. We first consider the marginal utility of holding numeraire. Following the previous denotation, $q_t = x_t + l_t$, and $n_t = w_t - q_t$. We obtain

$$MU_n(n_t) = -\mu_t + \min\left\{c_t - r_t, -(1-\alpha)\left(\frac{A_t u_t}{w_t - n_t}\right)^{\alpha}\right\} - \frac{\partial \Psi_t}{\partial n_t} - \frac{(w_t - n_t)\sigma_t^2 \partial_{ww} U}{\partial_w U}. \tag{A.22}$$

We want to show that for any positive $\epsilon < \bar{w}$, there exists $A_t(\epsilon)$ such that $MU_n(\epsilon) < 0$ for any $A_t > A_t(\epsilon)$. We have the following intuitions. First, $\frac{\partial P}{\partial A} \geqslant 0$. Since both transaction convenience and the aggregate amount of staking reward increases with A_t, a higher A_t will naturally attract more wealth from holding numeraire. Second, $\mu > -\infty$ based on the assumption that $\mu^A \geqslant 0$. A_t is a process that broadly captures technological advances, regulatory changes, and the variety of activities feasible on the platform, all of which suggest a fast and volatile growth of A_t. Suppose that μ_t tends to negatively infinity, then by Eq.(24), there must be $\frac{\partial^2 P}{\partial A^2} \to -\infty$, which contradicts the fact that the first order derivative is always greater than zero. This assumption follows Cong et al. (2021d), where the additional reasons for parameter choices also result in a bounded σ_t. Third, $\frac{w\partial_{ww} J}{\partial_w J}$ is bounded since it is a smooth function of $w \in [0, \bar{w}]$. Then $\forall \epsilon \in (0, w_t)$,

$$MU_n(\epsilon) < r^f - \mu - (1-\alpha)\left(\frac{Au}{w}\right)^{\alpha} + \psi(\epsilon) - \frac{w\sigma^2 \partial_{ww} U}{\partial_w U}, \tag{A.23}$$

where $\psi(\epsilon) = -\frac{\partial \Psi(\epsilon)}{\partial n} < \infty$. Let

$$A(\epsilon) = \max\left\{0, \frac{w}{u}\left(\frac{\psi(\epsilon) + r^f - \underline{\mu} + \bar{U}}{1-\alpha}\right)^{\frac{1}{\alpha}}\right\}, \tag{A.24}$$

where $\underline{\mu}$ and $\bar{U}$ are the lower bound of μ and upper bound of $-\frac{w\sigma^2 \partial_{ww} U}{\partial_w U}$ respectively, and the max term insures a non-negative A_t. Substituting $A(\epsilon)$ into Eq.(A.23), we obtain $MU_n(\epsilon) \leqslant 0$. Note that for the same ϵ, $MU_n(\epsilon)$ decreases with A_t. Therefore, $\forall A_t > A(\epsilon)$, $MU_n(\epsilon) \leqslant 0$. The result holds for any sufficiently small positive ϵ, which implies that when A_t tends to infinity, the marginal utility of holding numeraire is always negative. Therefore, all the wealth will be allocated to the platform, i.e.

$$\lim_{A_t \to \infty} V(A_t) = \int_W w_t m_t(w_t) \mathrm{d}w_t. \tag{A.25}$$

In the following, we summarize the steps of solving the pricing ODE Eq.(30). First, the equi-

librium Θ_t, r_t, and the integral equations for the crowd, are all functions of (A_t, μ_t, σ_t). Second, when substituting these functions into the market clearing condition, Eq.(26) will only contain P_t, μ_t and σ_t. Third, replacing P_t with V_t by Eq.(29) and apply to Itô's Lemma, we can express μ_t and σ_t by the derivatives of P_t. Then the equation implies a second-order ODE of $V(A_t)$ as Eq.(30) shows. As we mentioned, besides $V(A_t)$, $V'(A_t)$ and $V''(A_t)$, the remaining terms, including Θ_t, I_t, I_t^n and I_t^x are all functions of A_t. Therefore, in the process of numerical solution, we deal with a differential-algebraic system of equations (DAE) in fact. For the boundary condition, we choose a sufficient small ϵ and correspondingly choose $A(\epsilon)$ as Eq.(A.24) shows, so that $V(A(\epsilon)) \in (\int_W w_t m_t(w_t)\mathrm{d}w_t - \epsilon, \int_W w_t m_t(w_t)\mathrm{d}w_t)$. Let $V(A_t) = \int_W w_t m_t(w_t)\mathrm{d}w_t - \epsilon$ and calculate the solution. We then decrease ϵ until the new resulting solution is numerically indistinguishable from the previous solution. Finally, we substitute the solution of $V(A_t)$ and the differentials into Eq.(29) and Eq.(24) to obtain P_t, μ_t and σ_t, and then solve the equilibrium Θ_t, r_t, and the integral equations for the crowd.

A.5 Proof of Proposition 4

In Appendix A.2, we have proved that for any agents with different wealth, there is a unique q^* that satisfies the first order condition as Eq.(A.17) describes. Denote the excess return as λ_t, $\lambda_t = \mu_t + r_t - c_t$. Rearrange Eq.(A.17), we obtain

$$\lambda_t = -\frac{\partial \Psi}{\partial n_t} - \frac{q_t^* \sigma_t^2 \partial_{ww} U}{\partial_w U} + \frac{\min\{0, MU_x^* - MU_l^*\}}{\partial_w U}, \tag{A.26}$$

where MU_l^* and MU_x^* are marginal utility of staked and tradable tokens when agent's controls are optimized. Note that λ_t is a system state that is independent of the controls of a single agent, and the above equation holds for any w_t. Especially, for agents with zero staked tokens ($l_t^* = 0$), $MU_x^* \geqslant MU_l^*$, we obtain

$$\lambda_t = -\frac{\partial \Psi}{\partial n_t} - \frac{q_t^* \sigma_t^2 \partial_{ww} U}{\partial_w U}, \tag{A.27}$$

which can be interpreted as the trade-off between the transaction convenience of holding tradable token and the convenience of holding numeraire. Substituting into Eq.(A.26), we obtain they staked token is also compensated with staking rewards as financial returns for the loss of transaction convenience.

B. Extended Discussions

B.1 Comparative Statics: Wealth Distribution

In Section4, we obtain several implications under general wealth distributions. Especially in Figure 2 and 3, we use numerical solutions to illustrate the corresponding implications. To test that the results are robust with respect to different wealth distributions, we repeat the numerical simulation in multiple situations of m. As Appendix D. discusses, the baseline case in the main text is the Pareto distribution case, which captures the "80-20 rule" in practice that most wealth is held by a small group of people. For the comparative static, we also test two common cases, i.e. the normal distributions and the uniform distribution. The results are shown in Figure B1.

Subplot (A) repeats the implication that Figure 2 shows. All the curves have upward slope, which imply that agents stake more as the reward rate increase, although the specific paths differ somewhat due to the different wealth distribution. As for Proposition 2, the changes in the staking reward ratio can be intuitively represented as translations of the equilibrium line, while the corresponding equilibrium staking ratio is the intersect point of the upward staking ratio curve and the downward equilibrium line in Figure 2. It is obvious that the property hold for all the listed cases. Subplot (B) shows the joint dynamic of the staking ratio, Θ_t, and the price drift, μ_t, under different distributions. In general, the curves all have upward sloping trends, which imply the robustness that a greater staking ratio relates to higher expected prcie appreciation.

It is also interesting to think about the differences of the curves among different m. According to Subplot (A), an economy with more wealthy agents (e.g., $N(70, 5)$ compared to $N(30, 5)$) will have a higher equilibrium staking ratio (and a lower equilibrium staking reward rate at the same time). Subplot (B) implies that an economy with more wealthy agents will have a lower expected price appreciation under the same staking ratio. It is worth to point out that having more wealthy people in an economy is not equivalent to having more wealth concentrated in the the rich. The former may suggest that the economy contains a larger amount of total wealth. These phenomena generates a potential corroboration to the size effect of the platform growth and the price appreciation.

B.2 Comparative Statics: Emission Rate

In our model, a higher emission rate of token,ι_t, increases reward ratio, ρ_t, and thus is associated with higher staking ratio. The feedback effect of staking ratio generates a positive force on price appreciation. On the other hand, high emission rates lead to inflation, which are also expected by the agents as Eq.(33) shows. Therefore, with excessive emission rates, the feedback by high staking ratio may not be sufficient to compensate for price depreciation due to inflation.

Figure B2 shows the relationship between the system staking ratio, Θ_t, and the price dirft, μ_t, under different values of emission rate of token, ι_t. As the emission rate increases, on the one

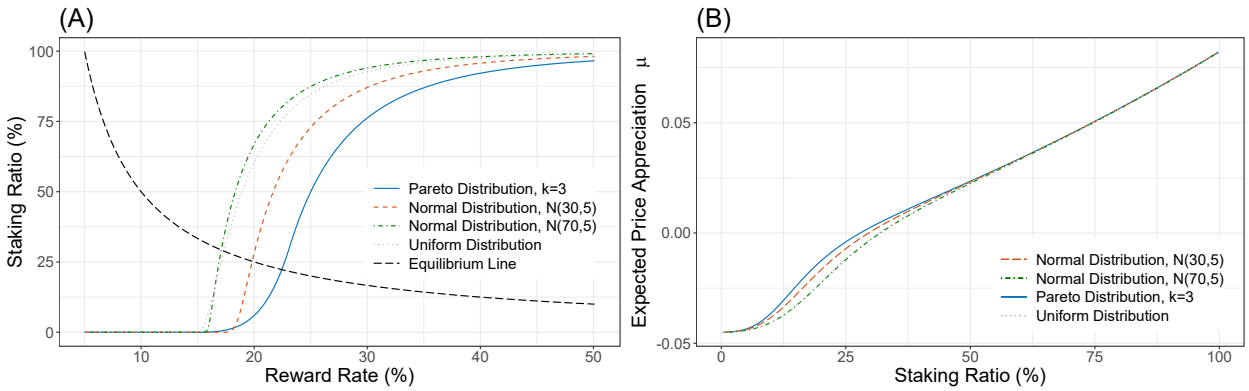

Figure B1: Comparative statics: Wealth distribution m.
This figure repeats the main implications that Figure 2 and 3 show, under different wealth distribution, m. We test four different cases, i.e., the Pareto distribution with parameters $w_{min} = 10$ and $k = 3$ (the benchmark case, the blue solid line), normal distribution $N(30, 5)$ (the orange dashed line), normal distribution $N(70, 5)$ (the green dotdashed line), and uniform distribution $U(10, 100)$ (the grey dotted line). Subplot (A) shows the overall staking ratio, $\Theta(m_t, r_t)$, as the blue curve in Figure 2 shows. The black downward curve draws the points that satisfies the fixed point problem (15). Since all the other global states are the same, the four cases share the same equilibrium line. The intersect points are the equilibrium situations $(r_t^*, \Theta(m_t, r_t^*))$ under corresponding m. Subplot (B) shows the relationship between the system staking ratio, Θ_t and the token price dirft, μ_t, as the blue curve in Figure 3 shows.

hand, the corresponding curves still have positive slopes, indicating the robust property that higher staking ratio relates to higher price drift. On the other hand, the overall downward shift of curves implies the impact of inflation. As the green dotted line shows, when the emission rate reaches 15%, the price depreciates even when the staking ratio is close to 1.

B.3 Robustness within PoS Tokens and DeFi Tokens

As Section 2 discusses, our model envolves both base layer pan-PoS staking mechanisms and higher layer DeFi stakable tokens. We model the common features and introduce several implications. In the empirical analysis, we use a sample containing the tokens from both the two layers. To empirically illustrate that these implications are common for both the pan-PoS and DeFi tokens, we divid our sample into two subsets based on the category of tokens, and repeat the main tests of each Table in Section 5 on the two subsets respectively.

Table B1 reports the results of these robustness tests. In Column (1), (2), we regress the staking ratio on the staking reward ratio $\rho_{i,t}$ in the same period as Table 2 does. The marketcap and volatility controls and time fixed effect are also considered. The estimated coefficients of $\rho_{i,t}$ are both significantly positive, which suggest the robustness within PoS tokens and DeFi tokens that higher staking reward corresponds to higher staking ratio.

Column (3), (4) test the regression as Column (6) of Table 3 reports. We regress the staking ratio on the reward rate $r_{i,t}$ in the previous week. The estimations for the two groups are consistent,

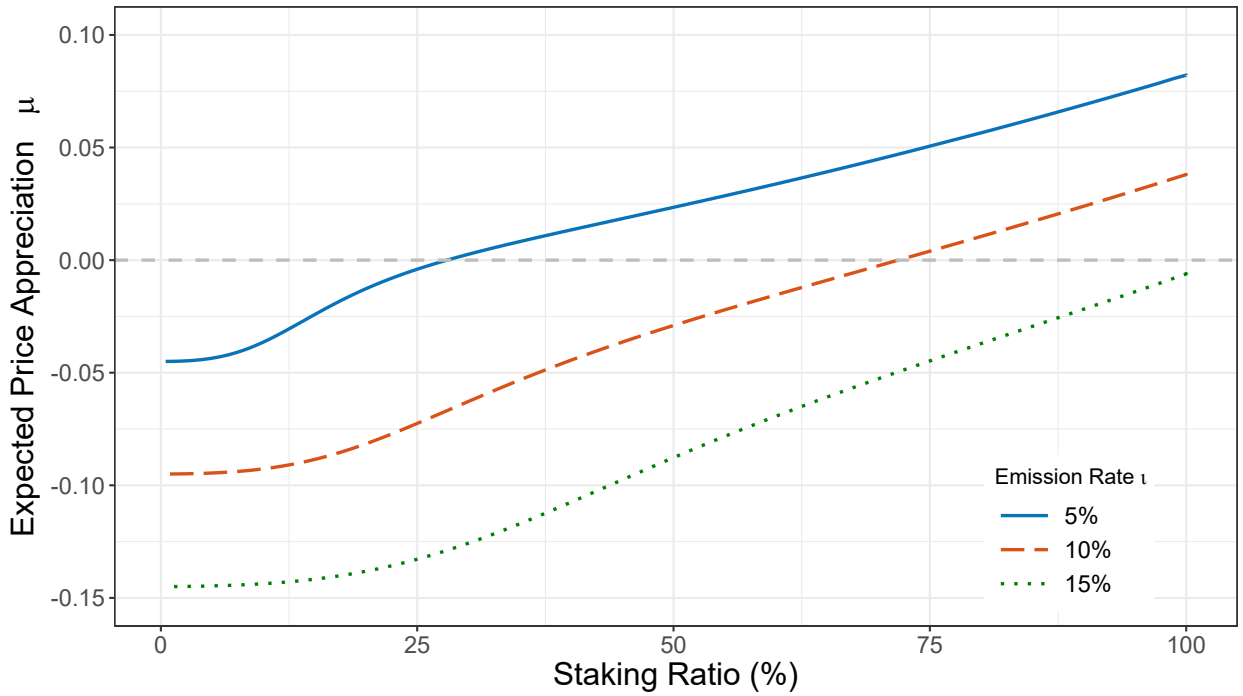

Figure B2: Comparative statics: Emission rate ι_t.
This figure shows the relationship between the system staking ratio, Θ_t, and the price dirft, μ_t, under different values of emission rate of token, ι_t. The values of other parameters are set according to Appendix D.. The blue curve shows the baseline case, $\iota_t = 5\%$, which is the same as the blue line in Figure 3.

and both implies that higher reward rate will attract agents to stake more.

Column (5),(6) test the regression as Column (5) of Table 4 reports. We regress the weekly log price change $r_{price_{i,t}}$ on the staking ratio in the previous week. The estimated coefficients of the staking ratio are both significantly positive and consist with our main empirical result, which suggest that the staking ratio predicts price appreciation. The performance of market and capitalization factors are both consist with related research.[38]

As a conclusion, our empirical tests for all three properties proves that the implications derived by our model apply to both pan-PoS and DeFi tokens.

C. Mean Field Game and the Master Equation

Mean field game (MFG for short), introduced in the pioneering works of Lasry and Lions (2007), is a powerful tool to analyze strategic interactions in large populations when each individual agent has only a small impact on the behavior of other players. MFG supposes that the rational agents are indistinguishable and individually have a negligible influence on the game, and that each individual

[38]Due to the limit of data, we have less than 100 sample points if the network term is included as control in Column (6). Therefore, we does not report the results within network term as control variable, although the corresponding test reports the consist conclusion.

Table B1: Robustness tests within two layers of tokens.

This table repeats the regression models of Tables 2, 3, and 4 on different subsets. As mentioned in Section 2, the in-sample tokens are divided into two groups, pan-PoS and DeFi tokens, based on their categories. Column (1), (2) repeat the model as Column (3) of Table 2 reports. Column (3), (4) test the regression as Column (6) of Table 3 reports. Column (5),(6) test the regression as Column (5) of Table 4 reports. These regressions are tested on pan-PoS and DeFi subsets respectively. t-Statistics are reported in parentheses. ***,**,* indicate statistical significance at the 1%, 5% and 10% respectively.

	$StakingRatio_{i,t}$		$\Delta StakingRatio_{i,t}$		$r_{price_{i,t}}$	
	PoS	DeFi	PoS	DeFi	PoS	DeFi
	(1)	(2)	(3)	(4)	(5)	(6)
$\rho_{i,t}$	1.146***	0.634***				
	(15.472)	(11.783)				
$\frac{1}{100}\log(\text{Cap})_{i,t}$	0.750***	2.242***				
	(4.289)	(7.522)				
$\text{Volatility}_{i,t}$	0.026	0.128				
	(0.208)	(0.681)				
$r_{i,t-1}$			0.028***	0.014*		
			(3.203)	(1.900)		
$\frac{1}{100}\log(\text{Cap})_{i,t-1}$			−0.016	0.023		
			(−0.173)	(0.164)		
$\text{Volatility}_{i,t-1}$			−0.001	0.017		
			(−0.033)	(0.468)		
$StakingRatio_{i,t-1}$					0.182*	1.121***
					(1.662)	(3.968)
r_{MKTt}					0.899***	0.460***
					(16.758)	(3.041)
$\log(Cap)_{i,t-1}$					−0.073***	−0.145***
					(−6.965)	(−4.569)
Fixed Effects						
Token			Y	Y	Y	Y
Time			Y	Y		
Observations	2,517	1,492	2,510	1,486	1,217	156
R^2	0.092	0.162	0.004	0.003	0.232	0.181

strategy is influenced by some averages of quantities depending on the states of the other agents. A very nice introduction to the theory of MFGs is supplied in the notes of Cardaliaguet (Cardaliaguet, 2010), including theoretical results on the existence and uniqueness of classical solutions, and also discussions on weak solutions.

MFG has a wide range of potential applications in economics. In macroeconomics, it has been applied to the studies that connects represent agent's optimization and the dynamic of macro interests, such as the income distribution (Achdou et al., 2022). It also allows heterogeneous settings, such as the heterogeneous-agent model (Krusell and Smith, 1998). Literatures also attempt to model financial problems using MFG. Brunnermeier and Sannikov (2016) compare the historical evolutions of macro-economic and finance models, arguing that properly framed, the analysis of continuous time stochastic models should provide a unifying thread for these sub-fields of economics which so far, developed in parallel.[39] To this end, the authors introduce models of the economy comparising households maximizing consumption like in classical macro-economic growth models, as well as investors trading in financial markets. Some applications have been discussed, including trade crowding (Cardaliaguet and Lehalle, 2018) and crypto mining (Li et al., 2019).

In many interesting situations in financial studies, it is important to allow for systematic risks (or systematic/common shocks). Such applications calls for a more general framework in theory. Fortunately, the MFG system can be written in the most general case in terms of a so-called "Master Equation" (Cardaliaguet et al., 2019). The Master equation is an equation on the space of measures, i.e. it is an equation that is set in infinite-dimensional space. The logic why the problem with aggregate uncertainty becomes infinite-dimensional is that the cross-sectional distribution across agents becomes a state variable in agents' dynamic programming problems and that distribution is an infinite-dimensional object.[40] The master equation is first introduced by Lions (2011). The most related research advances include the proof of the existence and uniqueness of a classical solution to the master equation (Cardaliaguet et al., 2019), monotonous solutions in several specific cases of common shocks (Bertucci, 2021), the case without idiosyncratic but with Brownian-type common shock (Cardaliaguet and Souganidis, 2020), and the corresponding weak solutions (Cardaliaguet and Souganidis, 2021).

D. Parameter Choices

In the numerical analysis, we set the initial wealth distribution to follow the Pareto distribution with parameters $w_{min} = 10$ and $k = 3$. Such distribution fits the trend that a large portion of wealth is held by a small fraction of the population. For numerical test, we set the maximum wealth to be $w_{max} = 100$, which is sufficient for discussion on heterogeneous optimal choice, and the corresponding value of cumulative function has already reached $1 - 10^{-3}$. Since there are unit measure of agents, the initial total wealth equals $\mathbb{E}(w) = 15$. We set the initial amount of tokens Q_0 to be 15, which makes the token price 1 approximately when all the wealth flows into the platform.

[39] This is also reviewed by Carmona (2020).

[40] This is also reviewed in the online Appendix of Achdou et al. (2022).

It is just to get a simple number without affecting any analysis process. For example, token price is halved when the total amount of tokens is doubled, while the equilibrium dynamics is invariant. We set the inflation rate ι fixed at 5%. The values are taken with reference to the actual issuance of tokens. On the one hand, the fixed value matches the setting of a large part of the tokens, that are designed to have a constant inflation rate, such as eos. On the other hand, the constant set makes the model easier to solve so that we can focus on the main interests. The rewards from transaction fee are defined as a random variable. Numerically, we exogenously set different values of τ ranges from 0 to 0.05. The resulting solutions satisfy Proposition 2. At the same inflation rate, larger τ leads to a larger amount of reward, and thus generates a larger equilibrium staking ratio and reward rate.

We set the annual risk-free rate of numeraire, r^f, constantly equals to zero. Then we choose $\mu^A(\Theta_t) = \mu_0 + \mu_1 \Theta_t^{\varkappa}$, where μ_0 represents the basic growth of productivity. As Cong et al. (2021d) discusses, A_t broadly captures regulatory changes, and the variety of activities feasible on the platform, which suggest a volatile growth of A_t. We set $\mu_0 = 0.5\%$ and $\sigma^A = 5\%$. We set $\mu_1 = 2\% > 0$ captures the positive contribution of staking as our model describes. The value of μ_1 also limits the maximum drift of μ^A to be 0.25% since $\Theta_t \leqslant 1$. We set $\varkappa = 1.5$ to feature the possible scale effect. It is not crucial for our main insights. We also test different values of $\varkappa$ such as 1 and 0.5, the key properties are not affected.

For parameters of agents, we set the instant utility to be $\mathcal{U}(y) = \frac{y^{1-\gamma}-1}{1-\gamma}$ with $\gamma = 0.9$, so that agents exhibit constant risk aversion $\gamma = 0.9$ the elasticity of intertemporal substitution $1/\gamma$. The discount factor ϕ is exogenously fixed to be 0.0099. The user type $U = U(w)$ reflects agents' transaction demand. We set $U(w) = \kappa w^{\delta}$ with $\kappa = 0.01$ and $\delta = 0.1$. This setting is to satisfy the natural assumption that $\frac{\partial U}{\partial w} > 0$, $\partial^2 U/\partial w^2 < 0$. The specific values taken have little effect on the main conclusions. For example, a larger κ makes the transaction convenience of all agents increases with constant A, but the direction and nature of the qualitative propositions does not change. We set $\alpha = 0.3$, which adjusts the sensitivity of the agent to the platform productivity. In Cong et al. (2021d), α is also set to be 0.3 to match the data. We set the participation cost, φ, to 0.001. With this value, we can completely observe the change of the adoption from 0 to 1. For the convenience of numeraire, we follow Valchev (2020) to model the consumption cost as $\Psi(y, n, A) = \overline{\psi}(A) y^{\beta} n^{1-\beta}$, where $\beta > 1$ features that costs are increasing in consumption, and decreasing in the level of numeraire holdings. We set $\beta = 1.2$ and $\overline{\psi}(A) = A^{-0.005}$, so that Ψ satisfies the assumption as A.4 discusses. In fact, in our study, the main impact of this term lies in the convenience gain of holding numeraire. With the guarantee that $\partial\Psi/\partial n < 0$, the specific choice of the relevant parameter does not affect the main properties.

E. Staking Mechanism of Tokens in Our Sample

In the following, we describe representative staking mechanisms of some tokens in our sample. Most information is accessed from *Stakingrewards.com*. There is also information from official websites of corresponding tokens. Many tokens have similar mechanisms, thus we do not repeat the description.

- The individual AION rewards depends on the Block Reward, Block Time, Daily Network Rewards and Total Staked. Every block one validator is randomly selected to create a block, whereas 1 staked or delegated token counts as one "lottery ticket". The selected validator has the right to create a new block and broadcast them to the network. The Validator then receives the 50% of the block reward and the fees of all transactions (network rewards) successfully included in this block, whereas the PoW Miner receives the other 50%.

- Rewards in the form of algos are granted to Algorand users for a variety of purposes. Initially, for every block that is minted, every user in Algorand receives an amount of rewards proportional to their stake in order to establish a large user base and distribute stake among many parties. As the network evolves, the Algorand Foundation will introduce additional rewards in order to promote behavior that strengthens the network, such as running nodes and proposing blocks.

- The individual BitBay rewards depends on the Block Reward, Block Time, Daily Network Rewards and Total Staked. Every block one staker is randomly selected whereas 1 staked coin counts as one "lottery ticket". The selected staker has the right to create a new block and broadcast it to the network. He then receives the block reward and the fees of all transactions successfully included in this block.

- Dash blockchain consensus is achieved via Proof of Work + Masternodes. Investors can leverage their crypto via operating masternodes. Miners are rewarded for securing the blockchain and masternodes are rewarded for validating, storing and serving the blockchain to users.

- Eos has a fixed 5% annual inflation. 4% goes to a savings fund, which might distribute the funds to the community later on. 1% goes to Block producers and Standby Block Producers. Out of the 1% that are given to block producers, only 0.25% will go to the actual 21 producers of the blocks. The other 0.75% will be shared amongst all block producers and standby block producers based on how many votes they receive and with a minimum of 100 EOS/day.

- The individual reward of staking fantom depends on the Total Staked ratio. Transactions are packaged into event blocks. In order for event blocks to achieve finality, event blocks are passed between validator nodes that represent at least 2/3rds of the total validating power of

the network. A validator's total validating power is primarily determined by the number of tokens staked and delegated to it. A validator earns rewards each epoch for each event block signed according to it's validating power. By delegating, investors can increase the share of their validator proportionally to the balance of their account. They will receive rewards accordingly and share them with investors after taking the commission.

- The effective yield for staking IDEX depends on the actual Trading Volume on IDEX Market. The higher the trading volume on IDEX, the higher are the actual rewards. The second metric to watch is the total amount of AURA currently staking. Less tokens on stake result in higher rewards.

- Every livepeer (LPT) token holder has the right to delegate their tokens to an Orchestrator node for the right to receive both inflationary rewards in LPT and fees denominated in ETH from work completed by that node.

- The individual LTO rewards depends on the Network Rewards (Transaction Fees spent on the Network) and the Total Staked. Every block one staking node operator is randomly selected to create a new block, whereas 1 staked token counts as one "lottery ticket". The staker receives the fees of all transactions successfully included in this block. Staking Node Operators share the rewards with their delegators after deducting a commission.

- NEM blockchain consensus is achieved via Proof of Importance. Investors can leverage their crypto via harvesting. To harvest NEM coins it is recommended to run the official NEM Core wallet with an entire copy of the blockchain on the stakers' computer or a Virtual Private Server (VPS). The individual NEM harvesting rewards depends on the Daily Network Rewards and Total Staked. Every block one staker is randomly selected whereas 1 staked coin counts as one "lottery ticket". The selected staker has the right to create a new block and broadcast it to the network. The staker then receives the fees of all transactions successfully included in this block.

- Everyone who holds NEO will automatically be rewarded by GAS. GAS is produced with each new block. In the first year, each new block generates 8 GAS, and then decreases every year until each block generates 1 GAS. This generation mechanism will be maintained until the total amount of GAS reaches 100 million and no new GAS will be generated.

- Nuls blockchain consensus is achieved via Proof of Stake + Masternodes. Investors can leverage their crypto via staking. The amount earned is variable based on the current blockchain metrics like the amount of stakers (Total Staked ratio). Investors can stake NULS into a

project's nodes and earn their token as a reward, while the project earns NULS as a reward. Some projects offer to stake with just 5 NULS as the minimum.

- Delegators in Polkadot are called Nominators. Anyone can nominate up to 16 validators, who share rewards if they are elected into the active validators set. The process is a single-click operation inside the wallet. The current reward rate for validators is determined by the current Total Staked ratio. The less DOT is being staked, the higher are the rewards.

- Qtum blockchain consensus is achieved via Proof of Stake 3.0. The individual reward depends on the Block Reward, Block Time, Daily Network Rewards and Total Staked. Every block one staker is randomly selected whereas 1 staked coin counts as one "lottery ticket". The selected staker has the right to create a new block and broadcast it to the network. The staker then receives the block reward and the fees of all transactions successfully included in this block.

- Synthetix Network Token blockchain consensus is achieved via the Ethereum Blockchain. Investors can leverage their crypto via staking. SNX holders can lock their SNX as collateral to stake the system. Synths are minted into the market against the value of the locked SNX, where they can be used for a variety of purposes including trading and remittance. All Synth trades on Synthetix Exchange generate fees that are distributed to SNX holders, rewarding them for staking the system.

- Tezos blockchain consensus is achieved via Liquid Proof of Stake. Investors can leverage their crypto via baking or delegating. There are a number of tokens that use a similar mechanism, including iotex, irisnet, etc.

- Tron reward depends on the Block Rewards, Endorsement Rewards, Block Time, Daily Network Rewards and Total Staked. Every block one staker is randomly selected to bake a block and 32 stakers are selected to endorse a block, whereas 1 staked coin counts as one "lottery ticket". The selected stakers have the right to create or endorse new block and broadcast them network. The Baker then receives the block reward and the fees of all transactions successfully included in this block. The Endorsers receive the endorsement rewards.

- Wanchain blockchain consensus is achieved via Galaxy Proof-of-Stake. The individual WAN rewards depends on the Foundation Rewards, Daily Network Rewards and Total Staked. At the beginning of each protocol cycle (epoch), two groups, the RNP (Random Number Proposer) group and the EL (Epoch Leader) group, are selected from all validators. 1 staked or delegated token counts as one "lottery ticket" to be selected. The two groups equally

share the Foundation Rewards and Transaction Fees (Network Rewards). The Foundation Rewards consists of 10% of the outstanding Wanchain Token Supply and are decreasing by 13.6% each year, whereas the Network Rewards are expected to rise alongside wider network usage.